
[All ETDs from UAB](#)

[UAB Theses & Dissertations](#)

2019

Identification Of Two Spop-Mediated Pathways In Prostate Cancer Progression

Joshua Fried
University of Alabama at Birmingham

Follow this and additional works at: <https://digitalcommons.library.uab.edu/etd-collection>

Recommended Citation

Fried, Joshua, "Identification Of Two Spop-Mediated Pathways In Prostate Cancer Progression" (2019). *All ETDs from UAB*. 1671.
<https://digitalcommons.library.uab.edu/etd-collection/1671>

This content has been accepted for inclusion by an authorized administrator of the UAB Digital Commons, and is provided as a free open access item. All inquiries regarding this item or the UAB Digital Commons should be directed to the [UAB Libraries Office of Scholarly Communication](#).

**IDENTIFICATION OF TWO SPOP-MEDIATED PATHWAYS IN PROSTATE
CANCER PROGRESSION**

by

JOSHUA FRIED

BO XU, CO-CHAIR
JIM, COLLAWN, CO-CHAIR
REBECCA BOOHAKER
JOHN PARANT
FRAN LUND
MARKUS BREDEL

A DISSERTATION

Submitted to the graduate faculty of The University of Alabama at Birmingham,
in partial fulfillment of the requirements for the degree of
Doctor of Philosophy

BIRMINGHAM, ALABAMA

2019

Copyright by
Joshua Fried
2019

IDENTIFICATION OF TWO SPOP-MEDIATED PATHWAYS IN PROSTATE CANCER PROGRESSION

JOSHUA FRIED

GRADUATE BIOMEDICAL SCIENCES – CANCER BIOLOGY THEME

ABSTRACT

Prostate cancer is one of the most common malignancies and causes of cancer related death in men. Morbidity is primarily attributed to late-stage and metastatic disease. Recent genomic screening studies have revealed that the Speckle type Poz Protein (SPOP) is the most frequently altered gene by missense mutations in prostate cancer. Interestingly, all of the identified mutations were located in the substrate binding domain of SPOP. Here, two pathways highlighting the impact of SPOP mutation on prostate cancer are presented. First, evidence showing that one of the naturally occurring SPOP mutations, serine 119 to asparagine (S119N), induces radiosensitivity and an apparent defect in the DNA Damage Response (DDR). The S119N mutant SPOP causes prolonged DNA repair, ineffective cell cycle checkpoints and reduced viability in response to ionizing radiation. Further, biochemical analysis of the functional significance of serine 119 demonstrated that it is required for radiation induced SPOP-ATM (Ataxia Telangiectasia) interaction. This is further validated by studies indicating that ATM, a critical mediator of the DNA damage response, is required for radiation induced serine 119 phosphorylation. In sum, the evidence shows that ATM phosphorylation of SPOP on serine 119 is a critical step in the DDR. Second, a clinical cohort of prostate cancer patients was analyzed and it was observed that SPOP mutation is an independent predictor of metastasis. Via proteomic analysis candidate proteins for SPOP regulation that also play a role in metastasis

were identified. It is demonstrated that SPOP interacts with and regulates ITCH protein levels. Further, the data indicates that SPOP mutation interrupts SPOP ITCH binding and leads to a subsequent accumulation of ITCH protein. Lastly, evidence demonstrated that increases in ITCH due to mutation in SPOP results in a concurrent loss of E-cadherin protein expression. Together are presented two clinically relevant SPOP-dependent pathways that impact prostate cancer initiation and progression.

Keywords: SPOP, Prostate Cancer, ITCH, ATM, DNA Damage, Metastasis

ACKNOWLEDGMENTS

I would like to first acknowledge my mentor, Dr. Bo Xu, for accepting me in to his lab. Dr. Xu provided monumental support, guidance, and encouragement as I worked on my project. His mentorship has improved my abilities in planning and conducting experiments, composing scientific literature, and giving oral presentations. Dr. Xu also encouraged me to broaden my horizons by attending large scientific conferences. Overall, thanks to Dr. Xu's mentorship I have grown as a scientist and am prepared to begin my own career in research.

Next, I would like to acknowledge the members of my committee, Dr. Fran Lund, Dr. Markus Bredel, Dr. John Parant, and Dr. Jim Collawn. Their expertise and criticisms was invaluable in both guiding and challenging me so that my project would be more productive and comprehensive.

Additionally, I would like to acknowledge lab members that have been instrumental in aiding me during my project. Especially, Dr. Rebecca Boohaker, and Dr. Qinghua Zeng. Both provided expertise on conducting experiments and were always willing to assist me in the lab. I would like to further thank Rebecca for her support as I was composing this thesis and finishing my time as a graduate student. Other lab members I would like to thank are Vinayak Khattar and Justin Avery. Also, I want to acknowledge the help from Stacey Kelpke and Lynae Hanks in editing my thesis.

I would also like to recognize Dr. Lalita Samant, theme director for Cancer Biology, for her efforts in aiding me as I finished my project and began writing my dissertation.

Lastly, I would like to acknowledge my parents for supporting me and providing for me throughout my life.

TABLE OF CONTENTS

	<i>Page</i>
ABSTRACT.....	<i>iii</i>
ACKNOWLEDGMENTS	<i>v</i>
LIST OF TABLES.....	<i>viii</i>
LIST OF FIGURES	<i>ix</i>
LIST OF ABBREVIATIONS.....	<i>xi</i>
BACKGROUND AND INTRODUCTION	<i>1</i>
A DISEASE-RELEVANT MUTATION OF SPOP HIGHLIGHTS FUNCTIONAL SIGNIFICANCE OF ATM-MEDIATED PHOSPHORYLATION IN DNA DAMAGE RESPONSE	<i>16</i>
SPOP REGULATION OF ITCH PROTECTS AGAINST PROSTATE CANCER METASTASIS BY MAINTAINING E-CADHERIN.....	<i>49</i>
DISCUSSION AND CONCLUSIONS	<i>70</i>
REFERENCES	<i>78</i>
APPENDICES	
A Approval for Animal Studies by Collaborator.....	<i>97</i>
B Approval for Human Studies by Collaborator.....	<i>99</i>

LIST OF TABLES

<i>Tables</i>		<i>Page</i>
BACKGROUND AND INTRODUCTION		
1	List of known SPOP substrates.....	4-5
2	List of SPOP alterations.....	6
A DISEASE-RELEVANT MUTATION OF SPOP HIGHLIGHTS FUNCTIONAL SIGNIFICANCE OF ATM-MEDIATED PHOSPHORYLATION IN DNA DAMAGE RESPONSE		
1	Proteins with increased abundance in lysates from SPOP pull down after radiation	41
2	Proteins with decreased abundance in lysates from SPOP pull down after radiation	42
SPOP REGULATION OF ITCH PROTECTS AGAINST PROSTATE CANCER METASTASIS BY MAINTAINING E-CADHERIN		
1	Primers used in sequencing.....	54
2	Clinical characteristics of 198 patients with prostate cancer included in the study.....	58
3	Localization and frequencies of SPOP mutations.....	59
4	Associations between metastatic reporting at first diagnosis and SPOP mutations.....	61

LIST OF FIGURES

<i>Figure</i>		<i>Page</i>
BACKGROUND AND INTRODUCTION		
1	Linear representation of SPOP with the location of prostate cancer mutants.....	2
2	Cartoon representation of SPOP binding with Cul3 and substrate	3
3	ATM involvement in cell cycle checkpoints	10
4	Schematic diagram outlining the functional roles of SPOP.....	11
A DISEASE-RELEVANT MUTATION OF SPOP HIGHLIGHTS FUNCTIONAL SIGNIFICANCE OF ATM-MEDIATED PHOSPHORYLATION IN DNA DAMAGE RESPONSE		
1	SPOP S119N mutation increases radiosensitivity.	27
2	SPOP Serine 119 mutation causes defects in the DDR.	28-31
3	SPOP Serine 119 is required for SPOP ATM IR induced interaction	32-33
4	SPOP is phosphorylated on Serine 119 after radiation in an ATM dependent manner.....	34-35
5	SPOP S119A mutation is similar to S119N mutation	36-37
6	SPOP S119N mutation causes γ H2AX accumulation in non-malignant prostate epithelial cells	38
7	SPOP S119 mutation causes radiosensitivity in prostate cancer xenografts in nude mice.....	39
8	Image of the protein gel that was submitted for mass spec analysis	40
9	DNA damage induces a SPOP complex that involves DNA repair and cell cycle regulatory proteins	43

10 SPOP interaction with MCM5 in response to IR.....45

SPOP REGULATION OF ITCH PROTECTS AGAINST PROSTATE CANCER
METASTASIS BY MAINTAINING E-CADHERIN

1 Actuarial analysis of all 198 patients63

2 SPOP regulates ITCH protein expression.....64

3 SPOP mutations abrogate binding with ITCH.....65

4 Mutation of SPOP down regulates E-Cadherin expression66

5 SPOP mutation increases cell migration.....67

LIST OF ABBREVIATIONS FOR KEY TERMS

ATM – Ataxia Telangiectasia Mutated

BTB – Bric a Brac Tramtrack Broad

CUL3 – Cullin3

DDR – DNA Damage Response

EMT- Epithelial to Mesenchymal Transition

γ H2AX – H2A histone family member X phosphorylated on serine 139

IR- Ionizing Radiation

ITCH – Itchy Homolog

MATH – Meprin and Traf Homology

S119N – SPOP serine 119 to asparagine mutant

S119A - SPOP serine 119 to alanine mutant

SPOP – Speckle Type Poz Protein

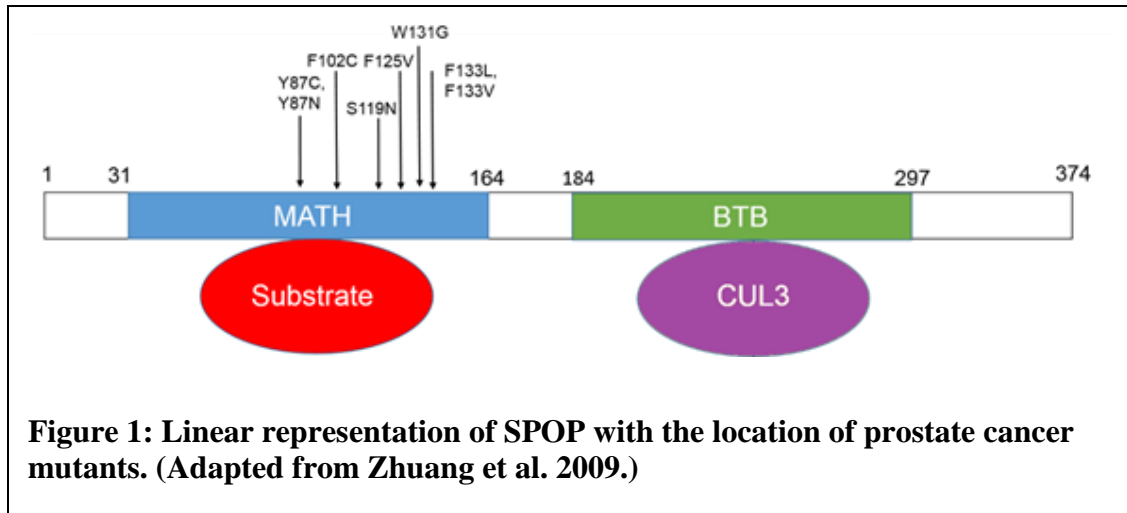
BACKGROUND AND INTRODUCTION

Introduction

Cancer initiation and progression are propelled, in large part, by the malfunctioning of critical cellular processes. These erroneous functions cause oncogenic phenotypes that can be classified into one of several categories, commonly referred to as the “Hallmarks of Cancer” (1). The Hallmarks of Cancer are driven by oncogenic aberrations in critical regulatory genes that give rise to altered expression of the subsequent expressed proteins, which are involved in the regulation of essential cellular functions. Additionally, these mutations often occur within the genome of a cellular lineage stem population, contributing to genomic instability in an entire tissue type. Of the Hallmarks of Cancer, genomic instability is often associated with more aggressive disease progression.

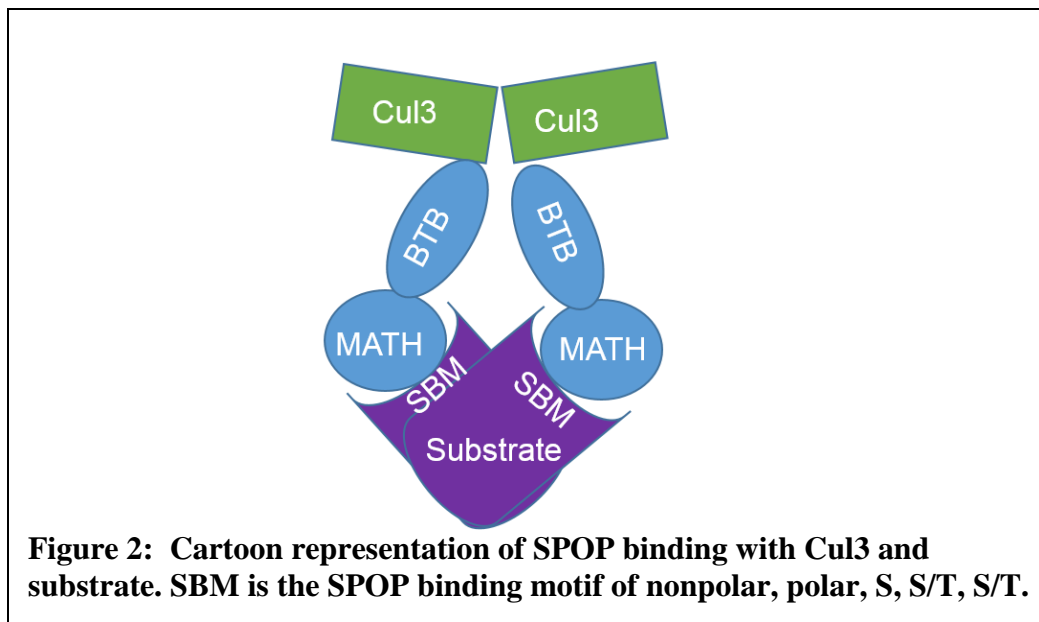
Mutations occurring with high frequency in diseased populations typically are either biomarkers or drivers of disease. Understanding the effects of oncogenic protein mutations within a tumor’s aberrant biology allows for the identification of disease, or even patient specific biomarkers, providing insight into the most effective therapeutic strategy within a disease subset. One such potential biomarker protein, the Speckle type POz Protein (SPOP), was discovered in 1997 by Nagai et al and named for the nuclear speckles it forms, as well as its homology to the protein-protein binding Poz domain (2, 3). Soon after its discovery, SPOP’s function as an E3 ubiquitin ligase adaptor protein was elucidated (4, 5). It was determined that SPOP’s canonical function revolves around its interaction with Cullin3 (CUL3) to mediate ubiquitination of target substrates. The theory that SPOP’s canonical function was tumor suppressive emerged from early studies identifying SPOP

substrates; many of which are known oncogenes (5-8). These studies suggested that SPOP mutation could result in a downstream dysregulation of critical oncogenic proteins and could contribute to disease progression. Indeed, meta-analysis of prostate cancer patient populations indicates that the gene encoding SPOP frequently bears mutations in critical domains (**Figure 1**), thereby affecting its function (2).



SPOP gene and protein

In 2009, Zhuang et al resolved the structure of wild-type SPOP, and determined that the protein is composed of 374 amino acids and two domains: an N-terminal Meprin and T-raf Homology (MATH) domain spanning residues 28-166 and a C-terminal Bric-A-Brac Tramtrak Broad (BTB) domain comprising residues 172-329 (9). The BTB domain facilitates the formation of a dimer-dimer complex with the CUL3 N-terminal domain. Through this interaction, SPOP participates in ubiquitination and protein degradation; whereas, substrate binding is mediated by the MATH domain (10, 11). The MATH domain is centrally located in a V-shaped groove composed by SPOP-CUL3 dimers. This dimeric structure allows for greater flexibility for binding and higher avidity for target substrates (**Figure 2**) (12).



Intriguingly, in prostate cancer a majority of the clinically observed mutations are localized to this domain (**Table 1**) (2). SPOP mutation in this domain leads to malfunction, accumulation of oncogenic substrates and potentially undiscovered downstream consequences resulting in tumor formation and progression. **Table 2** lists the previously identified SPOP substrates and their cellular function. Of interest in the work presented here, is the functional consequence of the clinically observed mutations within the MATH domain in the context of prostate cancer.

SPOP Substrates	
Protein Name	Protein Function
MacroH2.A	Chromatin Organization / Accessibility
PDX1	Insulin / Glucose Transport
Daxx	Transcription Repression / Apoptosis regulation
ERa	Hormone Signaling / Growth / Development
HHIP	Hedgehog Signaling / Development
Gli2/3	Hedgehog Signaling / Development
SRC3	Hormone Signaling
AR	Hormone Signaling / Growth / Development
SUFU	Hedgehog Signaling / Development
DUSP7	Tyrosine Phosphatase / Multiple Pathways
PTEN	Phosphatase / Metabolism
DDIT3	ER Stress
DEK	mRNA Processing
ERG	Transcription factor Multiple Pathways
SENP7	Senescence
PR	Hormone Signaling / Growth / Development

TRIM24	Transcriptional Control of Nuclear Receptors / Multiple Pathways
SETD2	Epigenetic Regulation
CDC20	Cell Cycle Regulation
Sirt2	Deacetylase
EgIN2	Oxygen Response
C-Myc	Transcription Factor / Multiple Pathways
INF2	Mitochondrial Dynamics
HDAC6	Epigenetic Regulation
BRD4	Chromatin Reader
PDL1	Apoptosis / Immune Response
MMP2	ECM regulation

Table 1: List of known SPOP substrates. The known SPOP substrates and the major cellular pathway that the substrate is involved in.

Description of SPOP Alterations in Different Cancer Subtypes	
Organ	Type(s) of Alteration(s)
Prostate	Missense Mutations, Loss of Expression
Endometrium	Missense Mutations, Loss of Expression
Breast	Loss of Expression
Brain	Loss of Expression
Colorectal	Loss of Expression
Gastric	Loss of Expression
Kidney	Overexpression, Cytoplasmic Localization
Liver	Missense Mutations
Ovary	Amplification, Deletion
Thyroid	Missense Mutations
Lung	Loss of Expression

Table 2: List of SPOP alterations. Table 2 lists the published SPOP alterations and the tissue where the alterations occur.

Canonical Function of SPOP and Implications in Prostate Tumor Suppression

SPOP binds to CUL3 via the BTB domain to form a complex for ubiquitinating target proteins (5). Ubiquitin (Ub) is a small regulatory protein that is covalently attached to target proteins, and labels them for proteosomal degradation (13). During the ubiquitination process, ubiquitin proteins interact with the substrate domain and Ub-E3 ligase, a substrate enzyme, to modulate the Ub system (14). E3 ligases can be grouped into the Really Interesting New Gene (RING) domain or the closely related U-box domain. The RING domain combined with the Cullin family can provide a scaffold for ubiquitin ligases (E3s) to form Cullin-RING ligases (CRLs) (15, 16). Ubiquitin ligases play an important role in maintaining genome stability and cell cycle control (17). Notably, control of the accumulation of cyclins and Cell Division Cycle 20 (CDC20), a substrate of SPOP, are crucial to maintaining the proper timing of the cell cycle and preventing aneuploidy.

In 2012, a critical tumor sequencing study demonstrated that SPOP mutation events were mutually exclusive with Transmembrane Protease serine 2-E26 Transformation Specific (TMPRSS2-ETS) gene fusion events, which occur in almost 70% of cases. These findings have since been supported by other tumor sequencing efforts (18-23). Taken together, these findings suggest that SPOP mutation may be an early event in prostate cancer tumorigenesis and that mutant SPOP is a potential driver of prostate cancer. Indeed, this hypothesis has been supported by *in vivo* data by two investigations showing that mutation or ablation of SPOP protein can lead to mouse prostate neoplasia (24, 25).

Further supporting the evidence of SPOP as a tumor suppressor is the steadily growing list of SPOP substrates, many of which are potent oncoproteins that have been shown to be differentially regulated at the protein level. Most prominent among these

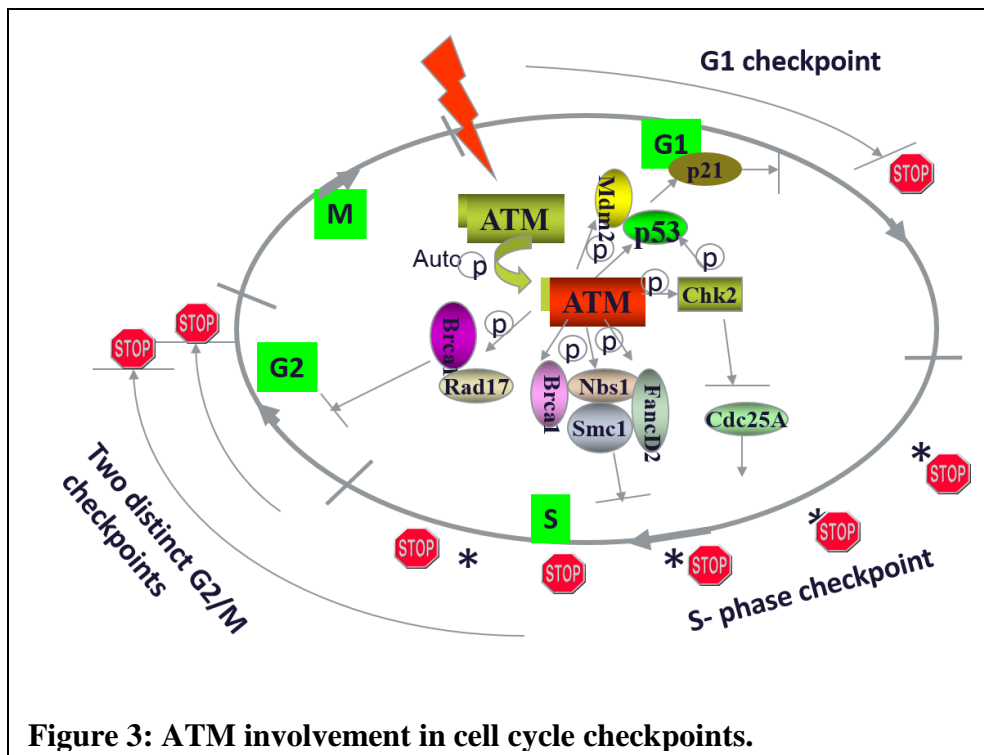
substrates in prostate cancer is the androgen receptor. In 2013 it was first verified that SRC3 is a SPOP substrate, and that SPOP mutants lost the ability to regulate Steroid Receptor Co-activator 3 (SRC3) resulting in aberrant androgen receptor (AR) activity (26). Additional evidence of SPOP's regulation of AR was then characterized in 2014, with a follow up study showing that SPOP can also directly regulate AR protein levels (27, 28). AR has been shown to be a critical driver of prostate cancer in both treatment naïve tumors and in post treatment "castration resistant" tumors (29). Another notable SPOP substrate is the ETS related gene (ERG) oncoprotein. ERG can be a potent driver of prostate cancer, even in the absence of a TMPRSS2 gene fusion (30). Multiple studies have shown that SPOP regulates ERG protein stability and degradation, and that SPOP mutation led to ERG accumulation, subsequently promoting an invasive phenotype (31-33). A study in 2014 demonstrated that SPOP, but not its mutant variants, ubiquitinates and promotes the degradation of a chromatin organizing protein, DEK proto-oncogene (DEK). It was shown that DEK accumulates in tumor samples bearing SPOP mutations (34). Other SPOP substrates suggest it plays a role in senescence, cell cycle regulation and histone modification (25, 35-41). The list of SPOP substrates is likely not complete, and will continue to grow as SPOP mutants are further studied.

SPOP's Emerging Role in the DNA Damage Response

Maintaining genomic integrity is crucial for the health and long-term survival at both the cellular and organismal level. Insults to DNA can come from both exogenous sources such as ionizing radiation (IR) and hazardous chemicals, or from endogenous sources such as reactive oxygen species (ROS) or even from self-imposed DNA damage during specific cellular processes (42-44). The DNA damage response (DDR) is a multi-

layered, highly regulated system of pathways that monitors, responds to, and corrects any aberrations to the genome (45). In addition to monitoring for damage to the DNA, the DDR is critical in cell cycle regulation checkpoints, halting progression at each transition to ensure incidental damage is not propagated to daughter cells (44, 45). The DDR employs multiple pathways; including but not limited to: base excision repair (BER), and nucleotide excision repair (NER) to resolve single strand breaks (SSBs) along with non-homologous end joining (NHEJ) and homologous recombination (HR) to repair double strand breaks (DSBs) (42, 46-50). As a therapeutic strategy, defects with the DDR, specifically the DSB repair pathways can be exploited with certain classes of chemotherapy or radiation therapy to critically damage cancer cells, but this carries the risk of collateral damage to non-cancerous cells (42).

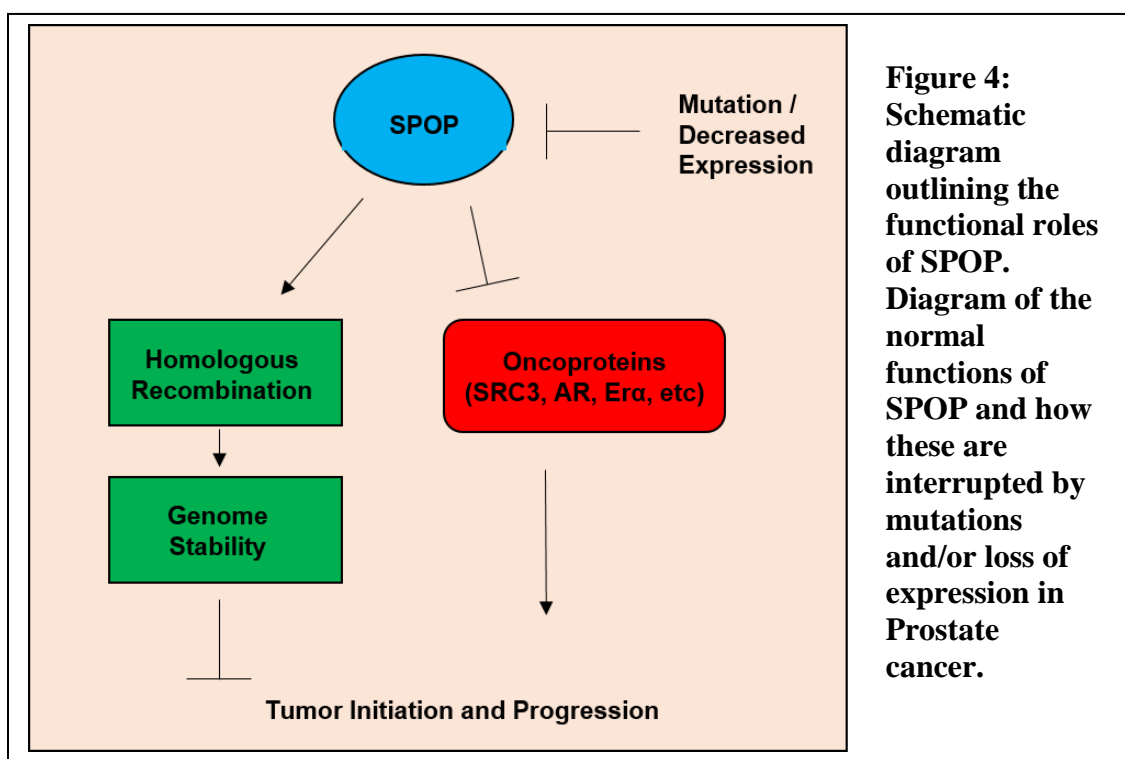
Central to the DSB response pathway is the ataxia telangiectasia mutated kinase (ATM), which serves as a hub protein to coordinate intracellular response to DNA damage (51, 52). Named for the disease caused by its mutation; ataxia telangiectasia (AT) causes the nominal symptoms ataxia and telangiectasia, (loss of body control and red patterning of the skin respectively) additionally, patients with this malady display increased radiosensitivity and a loss of DNA damage induced checkpoints (**Figure 3**). The subcellular consequence of the mutation typically exposes the affected person to higher genome wide mutation burden, genomic instability, and subsequent susceptibility to developing cancers (53-59).



ATM is a large, multi-domain protein with heat repeats and a C-terminal kinase domain (60, 61). ATM is recruited to sites of DNA damage by Nijmegen breakage syndrome (NBS1), a component in the Mre11, Rad50, NBS1 (MRN) complex via heat repeat binding (51, 52, 62). Once properly localized, ATM undergoes auto phosphorylation on S1981 and becomes active (63). Once active, ATM will then begin to phosphorylate a multitude of downstream effector proteins (51, 52). The ATM kinase domain recognizes target substrates via a consensus sequence XS/TQX (Serine, Threonine, Glutamine (Q), X any amino acid) flanked by hydrophobic or acidic residues (64). Chief among ATM's substrates is the histone protein, H2A histone family member X (H2AX). ATM phosphorylates H2AX on S-139 producing γ H2AX (65). Co-localization of γ H2AX with DNA lesions initiates a signaling cascade to repair damaged DNA (66). The list of substrates of ATM is ever growing, and the consequences of ATM phosphorylation span

across biochemical pathways from maintenance of cell cycle progression, to entering senescence, and even apoptotic signaling (67-70).

Currently, there are two reports that suggest SPOP has a role in the DDR. Preliminary work has shown that after DNA damage, SPOP interacts with ATM, and co-localized partially with γ H2AX as detected by confocal microscopy. Additionally, depletion of SPOP induced sensitivity to ionizing radiation (71). The other report demonstrated that SPOP mutants favor using the relatively error prone NHEJ DNA repair pathway opposed to the higher fidelity HR pathway (**Figure 4**) (72).



Together, these findings suggest SPOP is involved in the DNA damage response although the exact mechanism is not yet understood. Given the clinically observed S119N mutation within the MATH domain, the data contained within explores the significance of this mutation in the context of SPOP's role in the DDR.

Induction of DNA damage as a therapeutic strategy encompasses targeted ionizing radiation and DNA alkylating drugs such as the platinum class of drugs among others. The efficacy of these therapies is evident in their long and continued use as standard-of-care and frontline therapy (73). We sought to further explore SPOP function in the DDR via the putative ATM recognition site at S119 to elucidate the mechanism by which the SPOP-ATM interaction contributes to the response. SPOP interaction is significant enough in the context of genomic stability to provide an exploitable therapeutic target to induce radiosensitivity in tumors. Additionally, SPOP mutation could be used as a biomarker to identify patients where DNA damaging agents would be more effective.

SPOP, ITCH, and the EMT

The epithelial-mesenchymal transition (EMT), a process where epithelial cells acquire mesenchymal like properties, is used in development and wound healing by normal cells but is misappropriated by malignant cells during cancer progression (74-76). Epithelial cells are typified by strong cell junctions and well-defined cell polarity, whereas mesenchymal cells have increased mobility, invasiveness, and spindle like morphology (75, 77). EMT is driven by transcription factors Snail, Slug, Twist, and Zinc Finger E-box Binding Homeobox 1 (ZEB1), among others sometimes referred to as 'EMT-TFs', as well as differential expression of cadherin family members (78-80). EMT has also been shown to give cells a more stem phenotype in multiple cancer types (81-84). Evidence also shows that EMT contributes to tumor heterogeneity and resistance to chemotherapies. All of these complicate treatment of disease (85-87).

Metastasis is the primary cause of cancer related death across all subtypes (88). The metastatic process is complex and involves multiple steps, referred to as the "invasion-

metastasis cascade” (89-91). This process characteristically involves the invasion of surrounding tissues, intravasation into blood vessels, traveling to a new niche, extravasation, and finally, colonizing the new site. The EMT is integral to the metastasis cascade (76).

Analysis of our clinical data showed that presence of a SPOP mutation strongly correlated with metastatic prostate cancer. Proteomic screening of a cell culture model based on this analysis showed that the protein ITCH (AIP4 / Itchy homology) is a putative target for SPOP regulation. This was further evidenced by the presence of a SPOP target motif in ITCH’s amino acid sequence and additionally, by increased ITCH protein levels in lysates with depleted SPOP. ITCH, itself, is an E3 ubiquitin ligase that appends ubiquitin molecules to proteins often resulting in their destruction (92-94). Much of the literature describing the functions of ITCH denotes its role in the immune response. However, ITCH function is not limited to immune modulation.

Along with its role in the immune system ITCH ubiquitination activity has been shown to be involved in multiple cellular pathways; it is critical for the degradation of lipid soluble proteins giving an important role in lipid turnover (95-98). Additionally, ITCH is critical for the regulation of four potent proteins: JUN proto-oncogene (JUN), Cellular FLICE-like inhibitory protein (FLIP), Human Epidermal growth factor Receptor 2 (HER2), and Tumor Necrosis Factor (TNF) (99-111). Interestingly, there also exists evidence that ITCH promotes cell motility via down regulation of SMAD family member 7 (Smad7), a transcriptional regulator of Transforming Growth Factor β (TGF β), to promote EMT (112). Another study shows that ITCH down regulates Hippo function, thus increasing the oncogenic function of Yes Associated Protein (YAP) to promote

tumorigenesis by increasing cell proliferation, survival, and EMT (113). Involvement in the degradation of these proteins suggests that ITCH can be a tumor suppressor in certain contexts, and an oncogene in others. We hypothesize that the SPOP-ITCH regulatory axis is a major contributor to EMT in prostate cancer. Therefore, elucidating how SPOP impacts the EMT pathway via ITCH regulation is crucial to understanding SPOP mutation effects on tumor progression and metastasis.

Summary of works in this thesis

Presented in this work are two putative SPOP signaling pathways that provide insight into the significance of SPOP mutations in prostate cancer progression and metastasis. The first, shows the emerging role of SPOP in the DDR, first as a substrate of ATM and subsequently as a protein-level regulator of components of the DNA repair mechanism. The second, displays the more canonical function of substrate turnover regulation as a prostate cancer tumor suppressor.

The critical role of SPOP in the DDR is linked to an ATM recognition site at serine 119 in the MATH domain. This is a naturally occurring mutation site in the patient population. We determined the significance of this site through a series of radiation sensitization experiments on all clinically relevant SPOP mutants. Only one mutant, serine 119 to asparagine (S119N) caused increased radiosensitivity. This mutation also caused prolonged accumulation of γ H2AX, and a loss of the Gap2/Mitosis (G2/M) checkpoint. Additionally, S119N increased the percent of micronuclei positive cells after radiation. Next, SPOP's interaction with ATM was interrogated when serine 119 was mutated. Serine 119 mutation disrupted SPOP ATM binding, even in the presence of radiation induced DNA damage. Further, ATM could not phosphorylate SPOP if serine

119 was mutated. Next, the biochemical relevance of serine 119 was tested by using an alanine substitution instead of asparagine. Alanine substitution caused many of the same phenotypes of asparagine, demonstrating the relevance of ATM phosphorylation at this site. The *in vitro* data was then supported by *in vivo* data showing tumors expressing mutant SPOP were more radiosensitive than wild type expressing tumors in a murine model. Tumors bearing the S119N are likely to have a higher mutational burden due to defects in the DNA repair mechanisms, promoting oncogenesis and tumor progression.

In our study of the canonical function of SPOP as an E3 Ubiquitin ligase, a clinical analysis of a cohort of prostate cancer patients revealed that SPOP mutation correlated strongly with metastatic disease. A proteomic screen of lysates from prostate cancer cells with depleted SPOP was done to identify a novel SPOP substrate that also has a role in metastasis. ITCH was found to fit the above criteria and was chosen for validation and further study. Evidence showed that SPOP interacted with and regulated the levels of ITCH protein. Mutant variants of SPOP lost the ability to bind to and regulate ITCH protein. Depletion or mutation of SPOP decreased the protein levels of E-cadherin, an important regulator of EMT.

A DISEASE-RELEVANT MUTATION OF SPOP HIGHLIGHTS FUNCTIONAL
SIGNIFICANCE OF ATM-MEDIATED PHOSPHORYLATION IN DNA DAMAGE
RESPONSE

JOSHUA S. FRIED, JINLU MA, MINGMING XIAO, REBECCA J. BOOHAKER,
QINGHUA ZENG, AND BO XU

Submitted to Nucleic Acid Research

Format adapted for thesis

Abstract

The Ataxia-telangiectasia mutated (ATM) kinase phosphorylates a multitude of targets to facilitate the DNA damage response (DDR). Here, we report a prostate cancer-associated mutation of Speckle POz Protein (SPOP) and its impact in the DDR. We show that prostate cancer cells harboring the SPOP serine 119 to asparagine substitution (S119N) have prolonged DNA repair, an ineffective cell cycle checkpoint, and hypersensitivity to ionizing radiation (IR). We prove that serine 119 is required for SPOP interaction with ATM, and demonstrate that ATM phosphorylates SPOP serine 119 in response to DNA damage. The functional significance of ATM-mediated SPOP phosphorylation is demonstrated by both *in vitro* and *in vivo* evidence to regulate radiosensitivity, cell cycle checkpoints, and DNA repair. Further, we identified potential SPOP interactions in response to DNA damage. Taken together, we highlight a novel DDR pathway mediated by ATM phosphorylation of SPOP. These findings have clinical impact for prostate cancer patients as DNA damaging therapies may be particularly effective in this subgroup. This also provides the first evidence for a pathophysiological relevant mutation linked to ATM phosphorylation.

Keywords: SPOP, Prostate Cancer, ATM, DNA Damage Response

Introduction

Prostate cancer is the most common non-skin cancer in American men (114). Despite advances in both screening and treatment, it still remains a significant health risk (114). Genomic aberrations in prostate cancer include alterations of AR, p53, TMP ETS, and others (115, 116). A tumor sequencing study has shown that SPOP, an E3 ubiquitin ligase adaptor, is among these frequent mutations in prostate cancer (2). SPOP mutation has been demonstrated to be an early event in prostate cancer development (22). Interestingly, all of the cancer associated mutations occur in the substrate binding MATH domain (2, 9, 19). SPOP forms a complex with the CUL3 ubiquitin ligase (9), once bound to CUL3, SPOP mediates the ubiquitination and subsequent degradation of its substrates (9). Multiple substrates have been identified with many of them being known oncogenes, such as AR, SRC3, ERG, DEK, CDC20, and Bromo-domain containing 4 (BRD4) (8, 27, 33-35, 117). These findings, and others, posit that SPOP is a tumor suppressor in the prostate cancer setting. Although substrate regulation has garnered most of the attention, we and others have also shown that SPOP plays a role in the DDR (71, 72), and clinical data support the notion that SPOP mutation is associated with genomic instability (2). Further understanding SPOP's role in the maintenance of genome stability will provide insights into prostate cancer tumorigenesis and indicate a unique clinical outcome of a subgroup of patients.

The DDR is crucial for maintaining genome stability (45). An efficient DDR protects cells from both endogenous and exogenous genotoxic insults (45), and alterations in the genome are the cause of many cancers (1). The DDR is orchestrated by a comprehensive signaling transduction network which includes transcriptional regulation

and posttranslational modifications. Among the critical elements of the DDR network, ATM is the central regulatory kinase (63). Mutation in the *ATM* gene causes an autosomal recessive disease called Ataxia Telangiectasia, which is clinically manifested by progressive neurodegeneration, cancer predisposition, immunodeficiency and hypersensitivity to ionizing radiation and radiomimetic drugs (53, 55, 118) . As a serine/threonine kinase, ATM autophosphorylates itself and becomes active, upon detection of DSBs (63). Activated ATM phosphorylates numerous proteins to coordinate DSB repair. Despite extensive biochemical and cellular studies on ATM phosphorylation, these phosphorylation sites are rarely mutated in cancers, challenging the pathophysiological relevance of ATM-mediated phosphorylation in the disease setting.

In prostate cancer, SPOP serine 119 mutation to asparagine (S119N) is one of the clinically relevant mutations (2). Interestingly, we found that prostate cancer cells with S119N mutation possess a radiosensitive phenotype. In this report, we demonstrate the pathway and functional importance that links ATM and SPOP, highlighting the pathophysiological significance of ATM-mediated phosphorylation.

Materials and Methods

Cell culture

Prostate cancer cell lines PC3, DU-145 and LNCaP cells were purchased from the American Type Culture Collection (ATCC, Manassas, VA, USA). PC-3 cells were grown in DMEM supplemented with 10% fetal bovine serum (FBS) and 5% penicillin/streptomycin (P/S). DU-145 and LNCaP cells were grown in RPMI with 10% FBS, 5% P/S and 5% L-glutamine. LNCaP cells with tetracycline-inducible HA-SPOP expression were graciously provided by Dr. Nick Mitsiades (Baylor School of Medicine) (26). These cells were grown in RPMI with 10%FBS, 5% P/S, 5% L-glutamine, and 30 ug/mL G418 (Gibco, Dublin, Ireland). PWR1E prostate epithelial cell lines (ATCC) were grown in PREBM media supplemented with the nutrient bullet kit (Lonza, Mapleton, IL).

Irradiation

Ionizing radiation was delivered by an X-Rad 320 irradiator (Precision X-Ray Inc. N. Branford, CT, USA).

Antibodies and plasmids

Mouse anti-HA, and rabbit anti-GAPDH were purchased from Cell Signaling (Danvers, MA, USA). Rabbit anti-ATM, and rabbit anti- γ H2AX antibodies were purchased from Abcam (Cambridge, MA, USA). Rabbit anti α -tubulin was purchased from Sigma (St. Louis, MO, USA). The phospho-(Ser/Thr) ATM/ATR substrate antibody was purchased from Cell Signaling.

HA-tagged SPOP expression constructs including wild-type, Y87C, HA-F102C, S119N, W131G, F133L, F133V are all on the pcDNA 3.1 backbone and were provided by

Dr. Nicholas Mitsiades. The serine 119 to alanine mutation (S119A) was generated by site directed mutagenesis.

Transfection and induction of plasmids

Transient transfections were done using Attractene transfection reagent (Qiagen, Hilden, Germany), with an appropriate amount of DNA and serum free OPTIMEM (Gibco, Dublin, Ireland). The transfection reagent was used at a 3:1 ratio with DNA. The amount of DNA, transfection reagent and media were adjusted based on the amount of cells being transfected. 16 hours following the addition of the transfection mix, the serum free media was replaced with media supplemented with an additional 10% FBS. LNCaP cells were induced to express HA-SPOP constructs by the addition of 200ng/mL of tetracycline to the media for 48 hours.

Western Blotting

Protein lysates were electrophoresed across an SDS gel, and transferred to a nitrocellulose membrane. The membrane was blocked in 5% milk in TBST, and probed overnight at 4°C with appropriate antibodies. The membranes were then washed and probed for one hour at room temperature with secondary antibodies. Finally, membranes were incubated in developing solution (Thermo, Waltham, MA, USA) and developed onto film. Densitometry was done using Image J (National Institute of Health, Bethesda, MD, USA).

Micronuclei Quantification

The micronuclei staining kit was purchased from Intellicyt (Albuquerque, NM, USA). Cells were plated in 384-well plates at 3000 cells per well. The cells were then treated with radiation and fresh media was added 24 hours following radiation. 72-96 hours

following radiation the cells were stained according to the protocol. Cell sorting was done with the IQue (Intellicyt). Analysis was done using Forecyt software (Intellicyt).

Cell Cycle Analysis

Transfected cells were dosed with radiation and harvested 90 minutes following radiation. The cells were fixed in methanol overnight at 4°C. Fixed cells were then permeabilized with a solution containing 1% FBS and 1% triton-100 in PBS for 30 minutes. Permeabilized cells were probed with an anti-phospho H3 antibody conjugated to alexa fluor 488 (Cell Signaling). The cells were then washed and stained with propidium iodide (Molecular Probes, Eugene, OR, USA) for 30 minutes. Finally, the cells were sorted via a FACS Caliber (Becton Dickinson, Franklin Lakes, NJ, USA). Analysis was done using flowjo software.

3-(4,5-Dimethylthiazol-2-yl)-2,5-diphenyltetrazolium bromide (MTT)

Transfected cells were treated with increasing doses of ionizing radiation or left untreated. 24 hours following radiation all cells were supplemented with fresh media. 72 hours following radiation MTT (Acros Organics, NJ, USA), was added to the media in a 1:10 ratio. The cells were then placed back in the incubator until the MTT had been metabolized. PBS was then added to the media in a 1:10 ratio and the plates were kept overnight at 4°C while covered. Absorbance was read at 570nm by a Synergy 4 plate reader (Biotek, Winooski, VT, USA).

Colony formation assay

PC-3 cells were plated into six-well plates 24 hours after transfection in defined numbers. 24 hours following re-plating the cells were dosed with increased amounts of radiation. Fresh media was added after seven days. Once cell colonies had begun to reach

50 cells in size (10-14 days), colonies were fixed with 20% methanol. Following fixation the colonies were stained with crystal violet before the number of surviving colonies (>50cells) were counted.

Co-immunoprecipitation (Co-IP)

Cell lysates were pre cleared for four hours with a matrix from Santa Cruz. After pre clearing antibody was added along with species specific beads (Santa Cruz). The lysates were rotated overnight in 4°C with the beads and antibody. The bead lysate mixture was washed once with PBS and spun down. The supernatant was then used for immunoblotting.

In vitro kinase assay

In vitro kinase assay was done according to the protocol from Millipore. Briefly, 10 ng of purified constitutively active ATM (GenBank NM_000051) was incubated with 6 µM of wild type, S119N, or S119A SPOP peptide (Biomatik, Wilmington, DE, USA) of 10 amino acids in length or full length p53 in the presence of reaction buffer. 250 µM of ATP solution containing magnesium and manganese acetate was added to start the reaction. The reaction was allowed to proceed for one hour at room temperature. The reaction was stopped using ADP Glo reagents (Promega, Madison, WI, USA). Absorbance was read using a Synergy 4 plate reader (BioTek).

In Situ Proximity Ligation Assay (in situ PLA)

LNCaP cells were plated on to coverslips. Following induction cells were mock-treated or dosed with 5Gy of IR. Two hours following IR, coverslips were blocked and permeabilized with buffer from Duolink/Sigma. Then, cells were probed with mouse anti-HA and rabbit anti-ATM antibodies and stained with the Duolink PLA kit. Slides were

imaged with confocal microscopy (Nikon, Tokyo, Japan). Cellular PLA foci, which denotes an interaction, were counted for each experimental condition from at least five different fields of view.

In vitro binding assay

Binding assays were conducted using biolayer interferometry (BLI) on an OctetRed (Pall ForteBio, MenloPark, CA, USA) with Protein A labeled dip-and-read biosensors. Recombinant constitutively active ATM was loaded onto the biosensors at a concentration of 2ng/μl. Loading was done for 300 seconds (s), followed by a baseline reading then an association reading for 300s followed by a 600s dissociation reading. SPOP peptide concentration ranged from 0.740 to 60uM in 3:1 serial dilutions for initial binding experiments. Binding data was analyzed using the Octet software analysis system.

Stable Isotope Labeling of Amino Acids in Cell Culture (SILAC)

Lysate preparation: HA-tagged SPOP was expressed in DU-145 cells. Cells were grown for 5-6 generations in “heavy” medium. In parallel, untransfected DU145 cells were grown in “light” medium. HA-SPOP-DU145 cells were dosed with two Gy IR. Two hours following IR, cell monolayers from both heavy and light cultures were washed once with PBS and scraped into RIPA buffer at 0-4°C. The cell lysates from heavy and light cells were clarified by centrifugation for 15 minutes at 15,000 rpm and equivalent amounts of extract (determined by BCA assay, Pierce, Waltham, MA, USA) were added to yield approximately 4-5mg of total protein/mL and a final volume of 4mL.

Affinity beads: 500μl of HA agarose beads (Santa Cruz) suspension was washed once with medium salt (MS) buffer and mixed with 1mL of lysate (~ 5-7mg/mL) from light DU145 lysate. The beads were incubated for one hour at room temperature and washed

twice with MS buffer and once with high salt (HS). They were then resuspended in the original volume of MS buffer and used with the heavy/light lysate prepared as above.

Affinity purification: 100 μ L of pre-blocked HA agarose bead suspension was then added to 4mL of the heavy/light mixed lysates followed by rotation at 4°C for 2hr. The beads were centrifuged for 2 minutes at 2000 rpm and washed once with 15-20 volumes of 1 x CSK-NP and twice with 15-20 volumes of MS buffer. This was followed by resuspension of the beads in 300 μ L of HS buffer for 20 minutes at 0-4°C and centrifugation. Elution of the bait was carried out by incubation of the beads with 150-200 μ L of HA elution buffer. The supernatant is the HA-peptide eluate fraction (HA peptide fraction). Both, HS and HA-peptide fractions were subjected to MS analysis.

Mouse xenografts and lentivirus injection

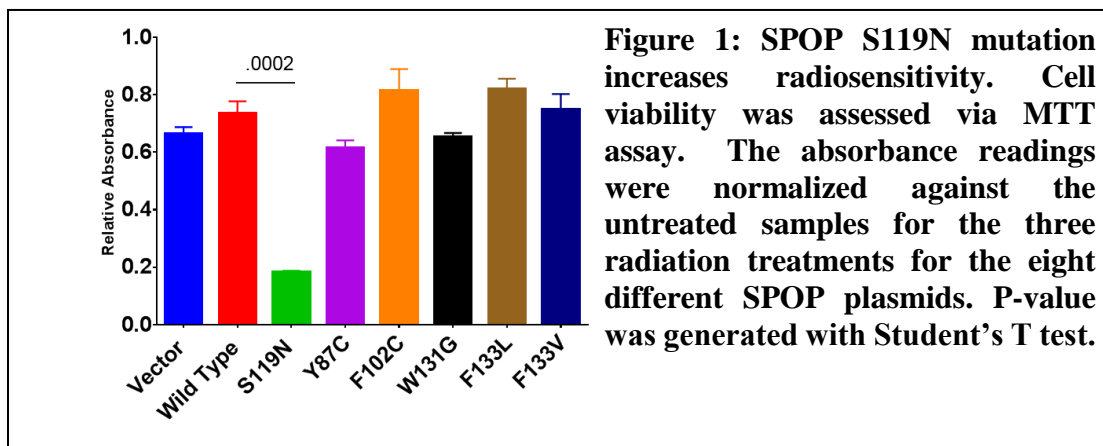
Athymic nude mice (4 weeks old) were purchased from the Beijing Experimental Animal Center and maintained in a specific pathogen-free facility approved by the Laboratory Animal Center of Xi'an Jiaotong University School of Medicine. For radiation re-growth delay studies, 1×10^7 LNCaP cells (mixed with Matrigel at a volume ratio of 1:1) were injected subcutaneously in the flank of the 4-week-old athymic nude mice. Tumor growth was observed every second day until the diameter of tumor reached 0.6 to 0.8 mm as measured by caliper. At this point animals were randomized into 8 groups (6 mice/group): control; IR; SPOP wt; SPOP S119A; SPOP S119N; SPOP wt + IR; SPOP S119A + IR and SPOP S119N + IR. Radiation treatment consisted of 10-Gy for 1 fraction. The mice were treated with lentiviruses respectively by carefully pipetting it on top of the epidermis covering the tumors in 100 μ l DMEM, lentivirus was administered twice per week. Three days post-injection, the mice were exposed to radiation. The length and width

of the treated tumors were measured using a Vernier caliper every two days. Tumor size was measured with calipers using the formula $V = (a \times b^2)/2$, in which a and b are the largest and the smallest perpendicular diameters, respectively. Tumors were followed individually until they measured greater than 800 mm^3 . The mean growth delay for each treatment group was calculated as the number of days for the mean of the treated tumors to grow to 800 mm^3 divided by the number of days for the mean of the control group to reach the same size.

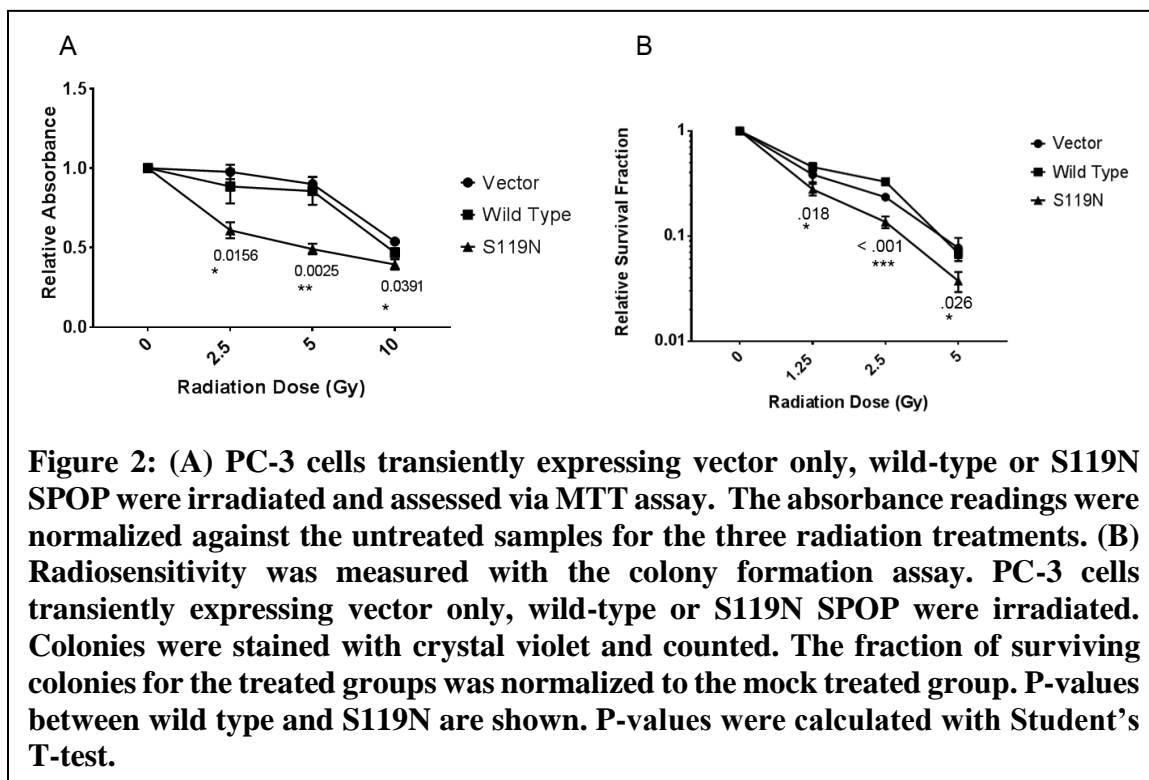
Results

SPOP S119N mutation impairs the DDR

Previous work and studies by others have demonstrated that SPOP plays a critical role in the DDR (71, 72), we theorized that SPOP mutations in the MATH domain have a distinctive cellular phenotype in response to IR treatment. We began our studies by assaying the radiosensitivity of prostate cancer cells expressing different SPOP mutants after being treated with IR. We tested a total of six mutations (Y87C, F102C, S119N, W131G, F133L, and F133V). Overexpression of wild-type SPOP reduced radiosensitivity, however, we found that only the S119N mutant caused a significant decrease in viability in response to IR (**Figure 1**).

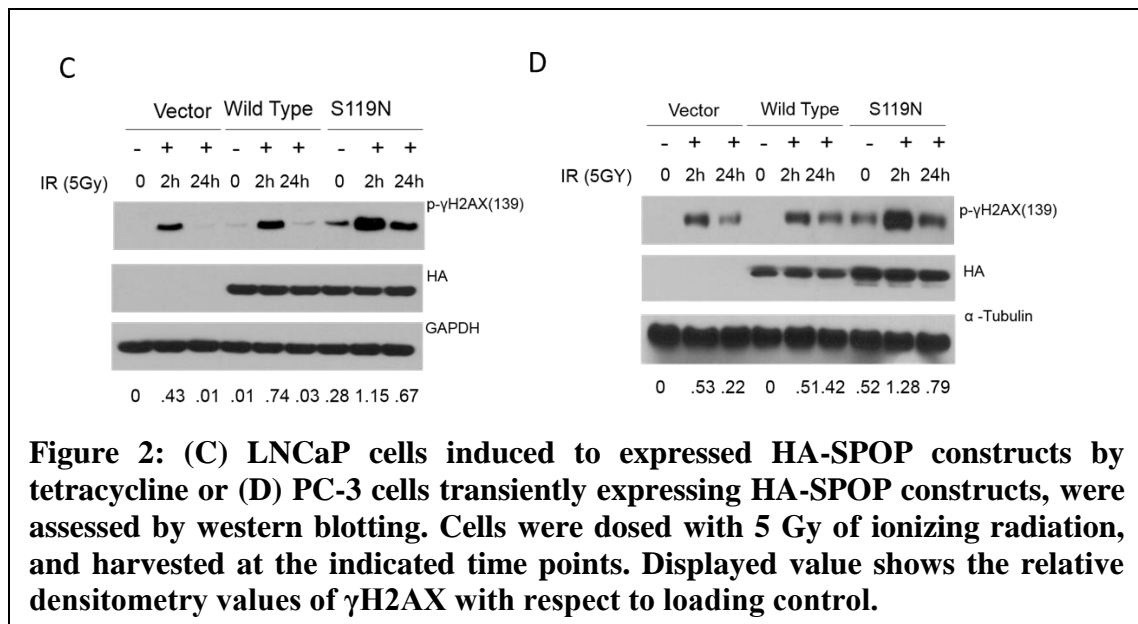


We then focused the remainder of our studies on this mutant. Both MTT and colony formation assay showed hypersensitivity to IR in cells expressing S119N (**Figure 2A and 2B**).

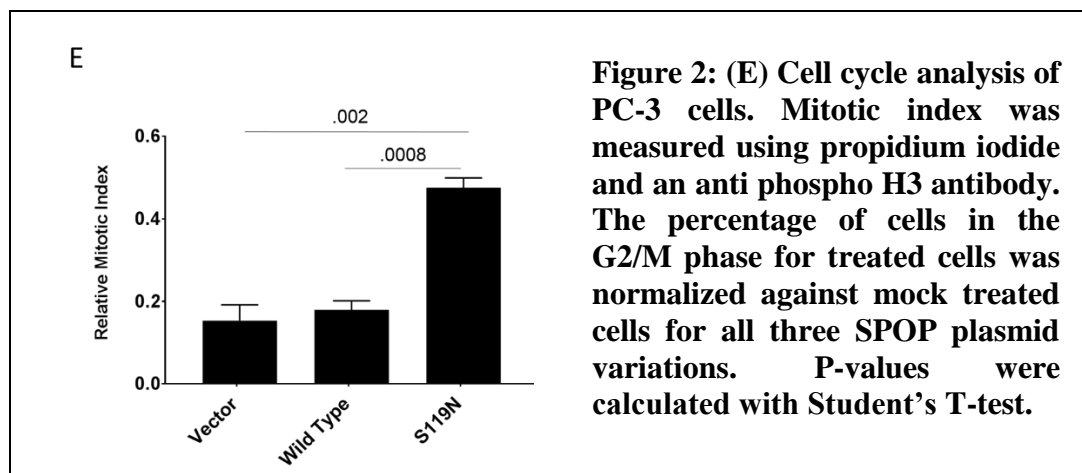


To further study the phenotypic defects in the DDR, we interrogated the timing of γ H2AX accumulation, a biomarker for an active DDR (119-121). γ H2AX can localize to DNA breaks in as early as a few minutes after the occurrence of DNA damage and is typically cleared within 24 to 36 hours following the genetic insult. We irradiated LNCaP and PC-3 cells expressing HA-tagged wild-type or S119N mutant of SPOP and assessed the γ H2AX levels via Western blot (**Figure 2C and 2D**). We found that the accumulation of γ H2AX in both the vector and wild-type SPOP expressing cells was greatly diminished 24 hours following IR. S119N expressing cells, however, noticeably retained higher levels of γ H2AX 24 hours after IR, suggesting that S119N mutation causes a reduced efficiency in DNA DSB repair. It is also noted that there was an increased level of γ H2AX even without radiation, implying that this mutation might impair the cellular response to endogenous

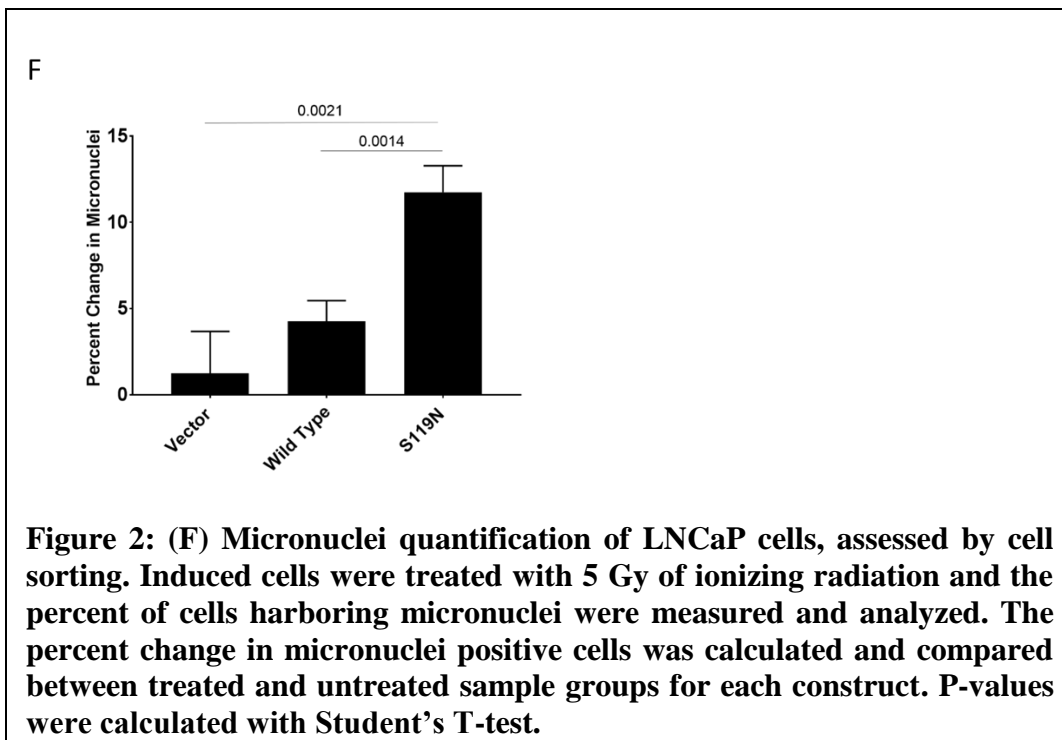
DNA damage. These results were consistent in both prostate cancer cell lines, PC-3 cells (transient expression) and LNCaP cells (tetracycline-induced).



Activation of cell cycle checkpoints is a critical step in the DDR, and impairment of the process is often associated with genomic instability and radiosensitivity (122-124). To investigate the impact that SPOP S119N mutation might have on cell cycle checkpoints, we measured cell cycle progression with propidium iodide and a phospho-Histone H3 antibody, a mitotic marker that can observe the G2 to M transition in the cell cycle. We found that cells harboring the S119N mutation had a significantly increased proportion of cells that were in the M phase of the cell cycle following radiation compared to that of vector or wild-type (**Figure 2E**), indicating a lack of the G2/M checkpoint.

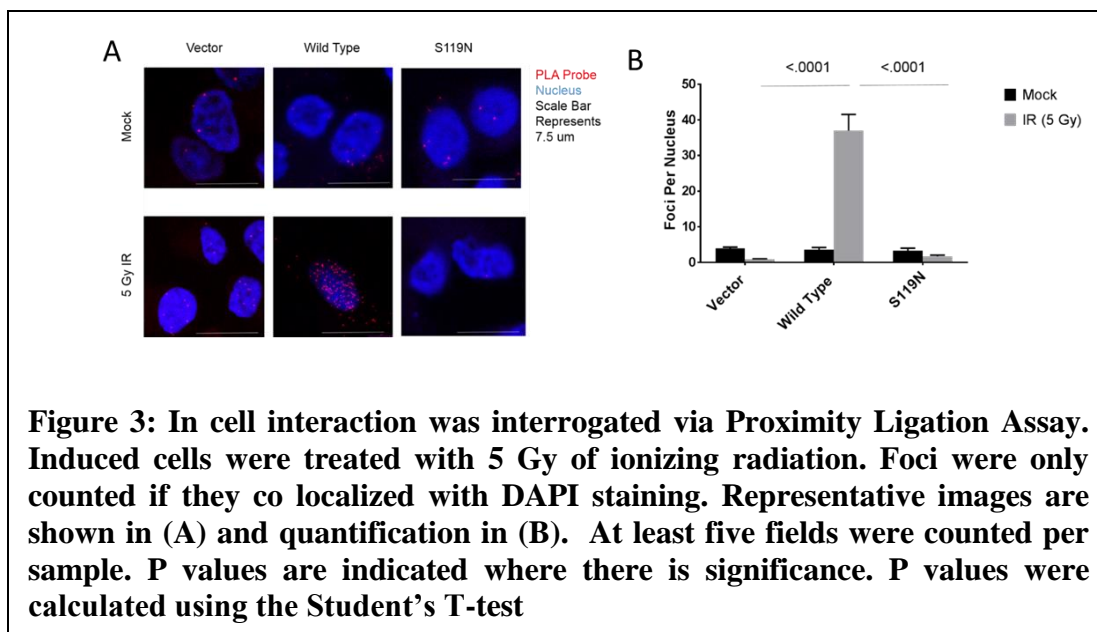


We then assessed if the faulty DNA repair mechanics caused by S119N had impact on genomic instability, measured by the number of micronuclei in response to IR. Micronuclei are formed during cell division when there is an abundance of unrepaired damage to the DNA (125, 126). We found that LNCaP cells expressing S119N mutant SPOP had a significant increase in the amount of micronuclei positive cells after IR, compared to vector or wild type expressing cells (**Figure 2F**). Taken together, our results indicate that S119N mutation causes abnormal DDR, hypersensitivity to IR and enhanced genomic instability.

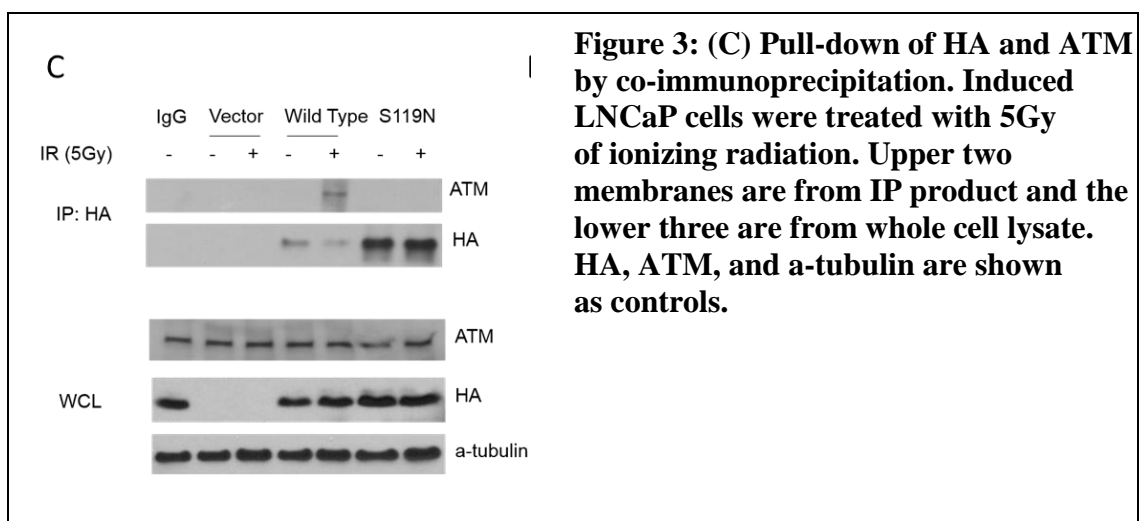


Serine 119 is essential for IR-induced SPOP- ATM interaction

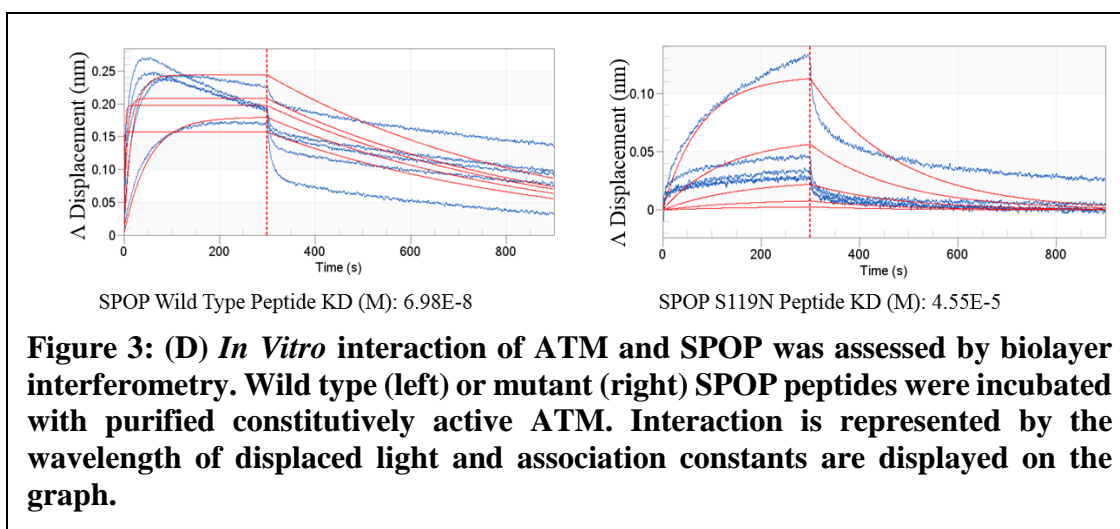
Previously, we have shown that SPOP and ATM interact in response to DNA damage (71). To test if the naturally occurring S119N mutation abrogates this interaction, we first used the *In Situ* Proximity Ligation Assay to query the interaction of ATM and SPOP. The reagents from this assay create foci that can be visualized with a confocal fluorescent microscope, the foci represent two different proteins or epitopes that are extremely close to one another, indicating interaction or co-localization. Mock-treated samples had very low numbers of foci. After IR, cells expressing wild-type SPOP had a substantially increased number of foci (**Figure 3A and B**). However, S119N expression significantly abrogated the formation of foci in response to IR, indicating that S119 is critical for the interaction of SPOP and ATM in response to IR.



After demonstrating that SPOP and ATM are in proximity to each other in the context of IR-induced DNA damage, we performed co-immunoprecipitation from prostate cancer cells expressing wild-type SPOP or S119N. The SPOP-ATM interaction is only observed after IR treatment and when wild-type SPOP is expressed (**Figure 3C**). S119N SPOP failed to co-immunoprecipitate with ATM. Taken together, these data further support that the SPOP-ATM interaction in response to DNA damage is dependent on serine 119.



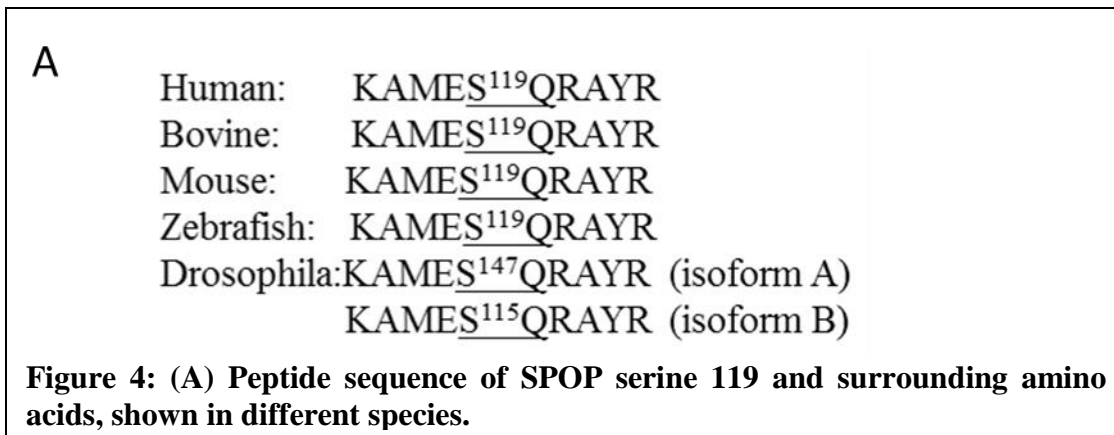
To test if the serine to asparagine substitution would interrupt binding directly in an *in vitro* system, we measured SPOP-ATM binding using biolayer interferometry (BLI) (127) and tabulating the results with the OCTET Red interferometer. Increasing concentrations of wild-type SPOP peptides or S119N mutant SPOP peptides of 10 amino acids in length were incubated with full length ATM (recombinant). The wild-type peptide had roughly double the amount of peptide bound to ATM than the mutant peptide as measured by diffracted light wavelength (**Figure 3D**). Additionally, we quantified the K_d values of the different peptides. The mutant peptide had a K_d value over 100 fold higher than the wild-type peptide, demonstrating that the mutant dissociated more easily from ATM. Taken together, S119N decreased binding to ATM and increased dissociation from ATM.



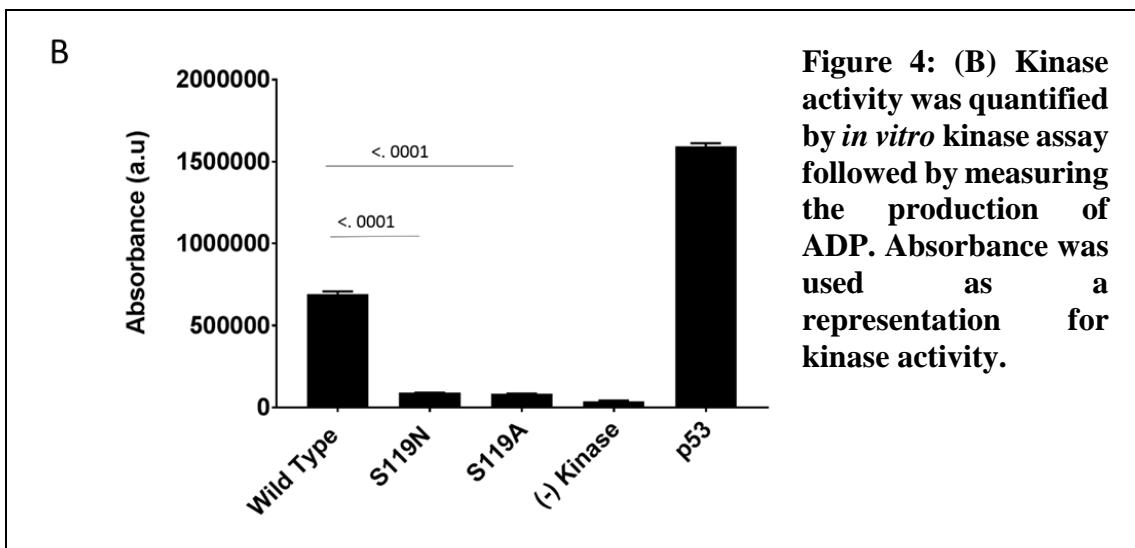
ATM phosphorylates SPOP on Serine 119 in response to IR

As a serine/threonine kinase, ATM recognizes the S/T-Q consensus motif for substrate phosphorylation (128). There are three potential sites (Threonine-T25, S119 and T319) in SPOP that meet the criteria of the SQ/TQ sequence. However, only S119 fully meets the criteria in the SQ surrounding sequence: 1. Hydrophobic amino acids at N-1, N-

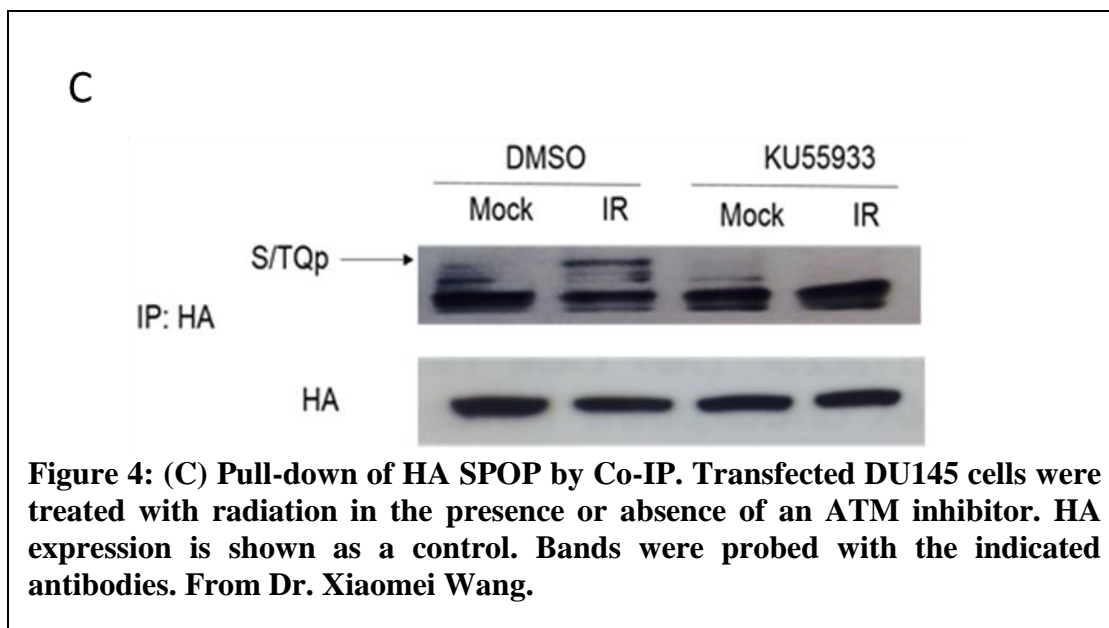
3 with exception of P/M/Y/G/F and S/A/D/E at N-3 and N-1, and 2. No positively charged residues around the target SQ, which might inhibit substrate recognition. Molecular modeling has obtained structural insight of serine 119 (9). It is also noted that that S119 is well-conserved across species (**Figure 4A**).



To test the potential for direct phosphorylation, we first performed an *in vitro* kinase assay, in which active ATM (recombinant) was incubated with wild-type, S119N, or S119A (serine to alanine mutant) SPOP peptides. We found that mutation on S119 caused a dramatic reduction in phosphorylation signals (**Figure 4B**). Conversely, the wild-type peptide displayed noticeable kinase reaction. These results indicate that S119 of SPOP can be phosphorylated by the ATM kinase.



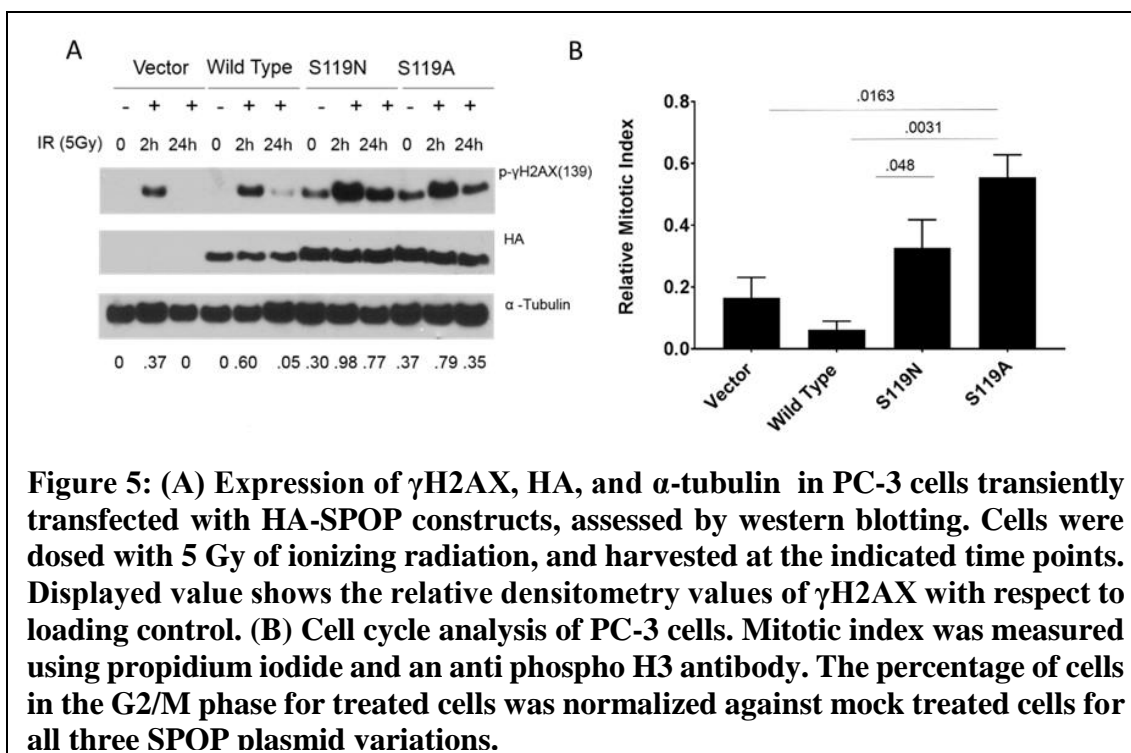
To assess potential phosphorylation in cells, we pulled-down HA-tagged SPOP and probed with an anti-phospho- S/TQ antibody for ATM phosphorylation. We found that S/TQp can be detected only in samples that had been irradiated. Meanwhile samples that had been irradiated but were also treated with the ATM inhibitor KU 55933 did not form this upper band, suggesting an ATM-dependent S/TQ phosphorylation in SPOP (**Figure 4C**).



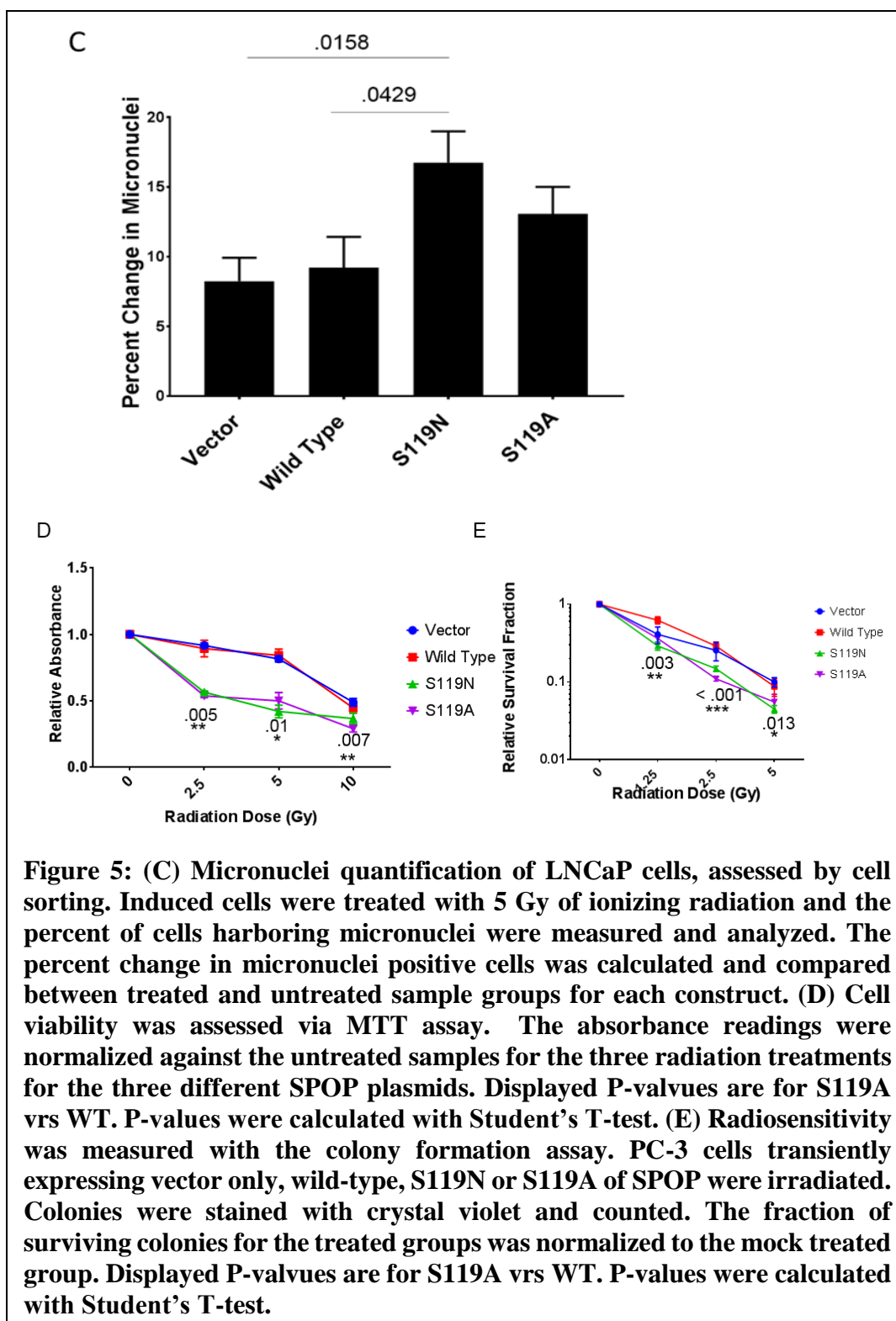
SPOP S119A mutation recapitulates S119N mutation

The SPOP S119N mutation is one of the naturally occurring SPOP mutations in prostate cancer. However, we wanted to enforce our hypothesis that the radiosensitive phenotype caused by S119N is caused mostly by the disruption of phosphorylation and not by possible conformational changes that an asparagine substitution would cause. To accomplish this, we utilized an alanine substitution (S119A) which would block phosphorylation but would not cause conformational changes as an asparagine substitution (S119N) might. We expressed these mutant proteins in PC-3 cells and measured cellular responses to IR. We found that similar to S119N, S119A mutation caused prolonged

γ H2AX accumulation after IR and also increased the levels of γ H2AX even in cells that received mock treatment (**Figure 5A**). Meanwhile, the S119A mutant caused a loss of the G2/M checkpoint (**Figure 5B**).

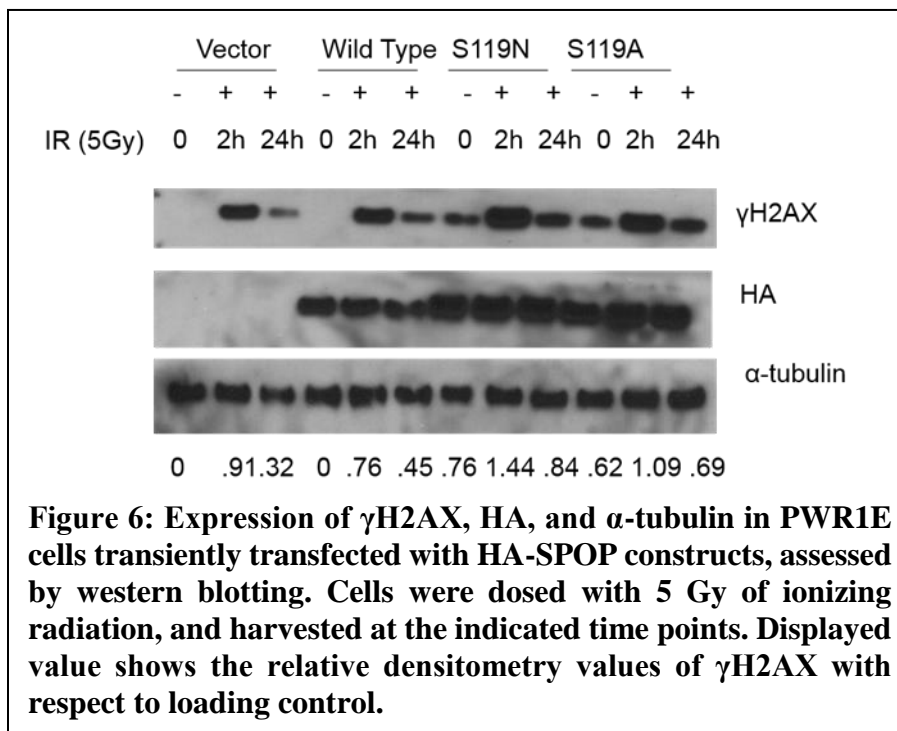


S119A mutation also caused an increase in micronuclei, although the statistical difference was not significant ($p=0.09$ with vector) (**Figure 5C**). We also found that cells expressing the S11A mutant showed hypersensitivity to IR, a similar phenotype as the S119N mutant (**Figure 5D and 5E**). Taken together, we conclude that ATM-phosphorylation of SPOP on serine 119 is critical for activation of the DDR and regulation of radiosensitivity.



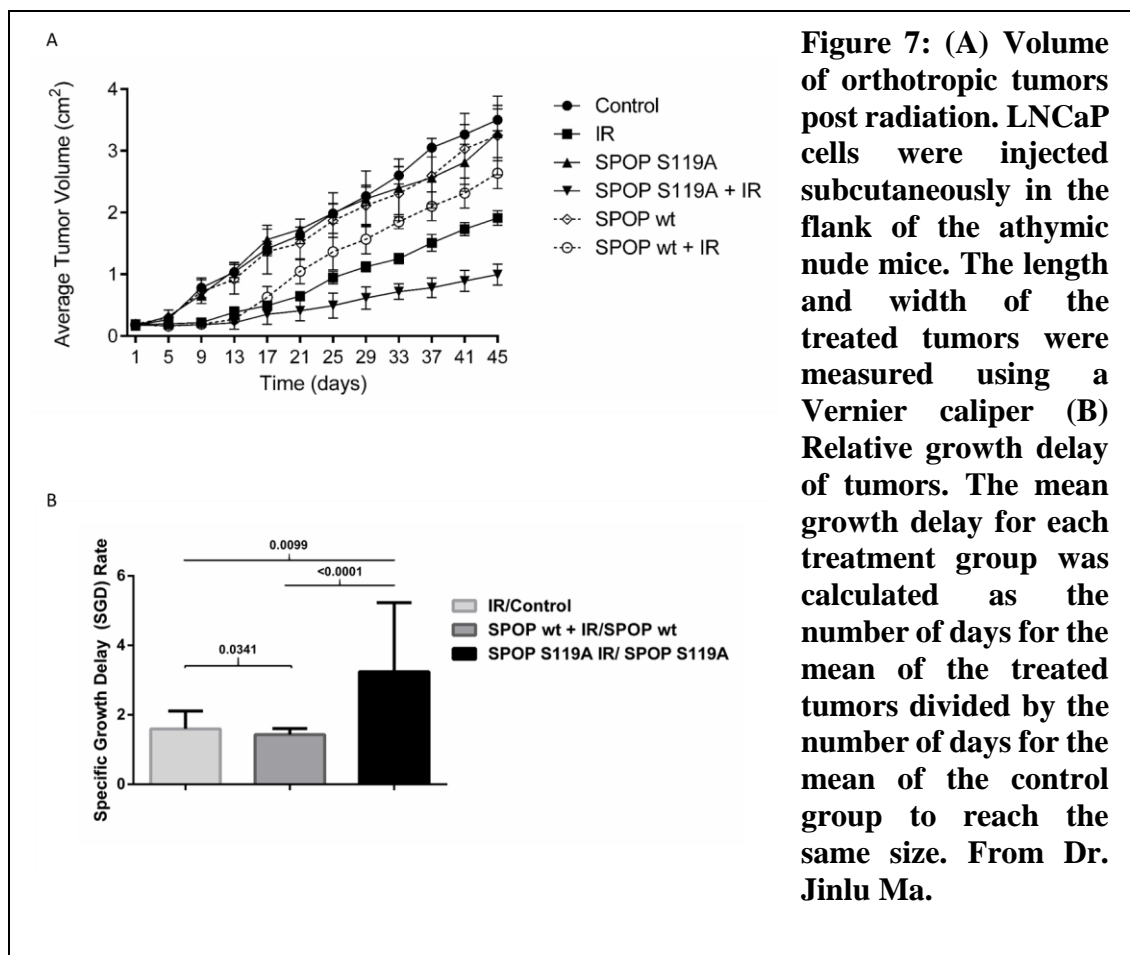
S119N or S119A causes genomic instability in nonmalignant prostate epithelial cells

So far, the models we have used have been prostate cancer cell lines; which might have a confounding effect when studying genomic instability. We wanted to discern if SPOP serine 119 mutation could cause disruptions in the DDR in nonmalignant prostate epithelial cells. To reach this goal, we transiently transfected PWR1E (nonmalignant prostate epithelial) cells with wild-type, S119A, S119N SPOP or an empty vector. We treated the cells with IR and assessed the clearance of γ H2AX. We found both S119A and S119N mutants caused delayed clearance of γ H2AX and accumulation of γ H2AX even without radiation treatment (**Figure 6**), supporting the conclusion that SPOP serine 119 mutation can lead to genome instability in non-cancerous prostate epithelial cells.



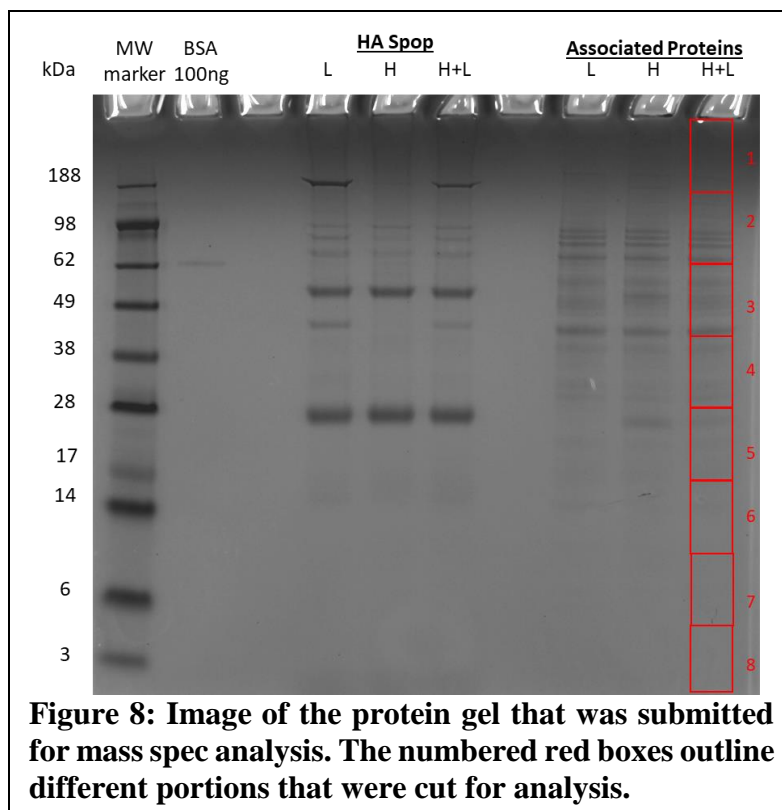
SPOP S119 mutation causes radiosensitivity in prostate cancer xenografts in nude mice

To strengthen the conclusion on the functional significance of ATM phosphorylation of serine 119, we conducted radiosensitivity experiments for prostate cancer xenografts in athymic nude mice. For radiation re-growth delay studies, LNCaP cells stably expressing vector only, wild-type or S119A were mixed with matrigel and injected subcutaneously in the flanks of mice. We found that xenografts expressing S119A were significantly more sensitive as compared to wild-type or vector (**Figure 7A**). The specific tumor growth delay rate for S119A is 2.7 (p=0.0001, compared to wild-type) (**Figure 7B**). These results strongly support that ATM-phosphorylation of SPOP on serine119 is critical for reducing radiosensitivity.



DNA damage induces a SPOP complex that involves DNA repair and cell cycle regulatory proteins

To further elucidate SPOP's function in the DDR, we aimed to identify proteins that SPOP interacts with upon IR. To achieve this goal, we first performed Stable Isotope Labeling by Amino acids in Cell culture (SILAC) with HA-tagged SPOP expressed in DU145 cells. We submitted gel portions containing samples from salt washes for mass spec analysis to identify potential SPOP interacting proteins (**Figure 8**). By measuring the abundance of peptides in the gel bands, we determined if proteins had an interaction with SPOP that was induced, abrogated or unaffected by IR treatment. We then categorized these proteins based on whether or not the interaction with SPOP was increased (**Table 1**) or decreased (**Table 2**) upon radiation treatment.



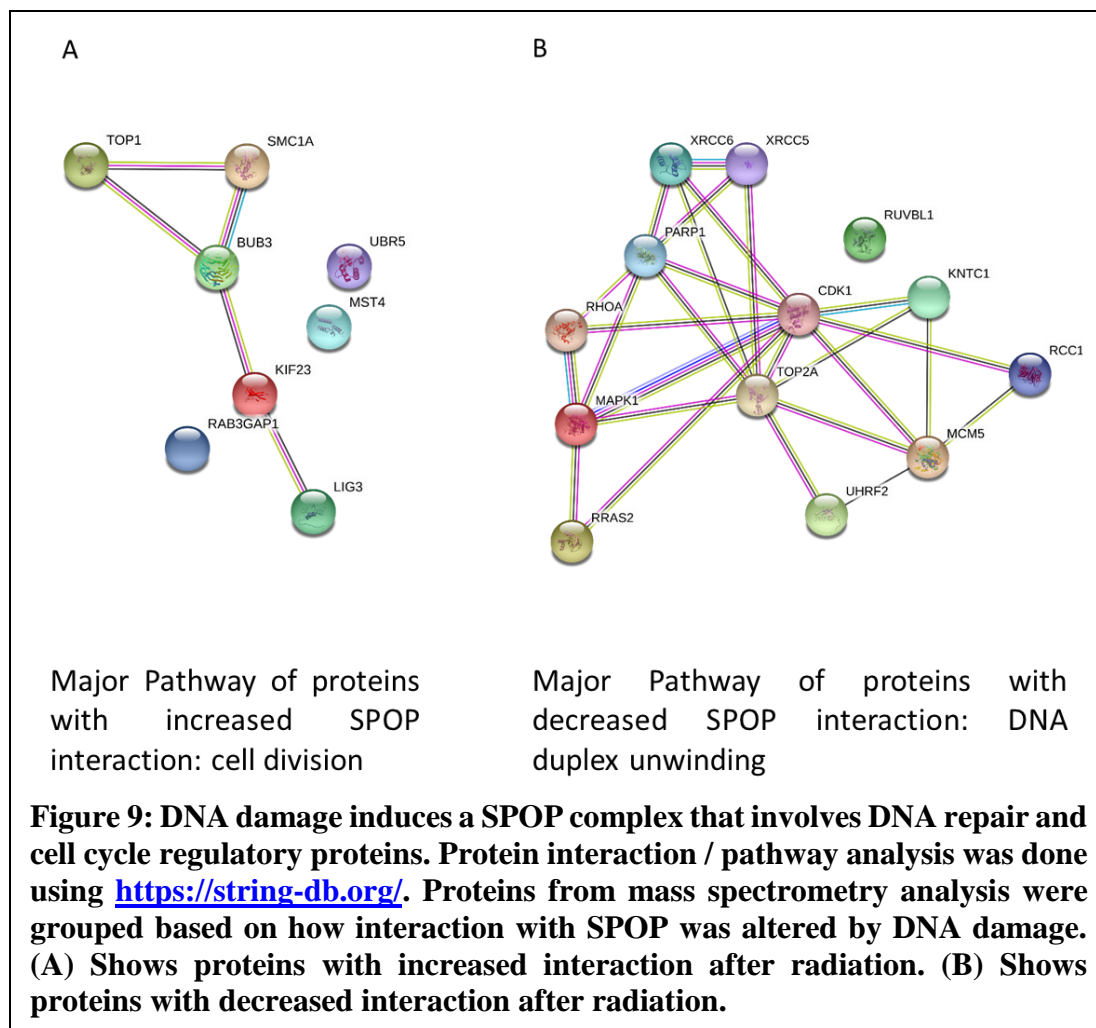
DNA Damage Proteins With Altered SPOP Interaction	
After Radiation	
Protein Name	Change
DNA Topoisomerase 1	Increase
SMC1a	Increase
UBR5	Increase
DNA Ligase 3	Increase
DNA Topoisomerase 2	Decrease
MCM5	Decrease
PARP1	Decrease
XRCC5	Decrease
XRCC6	Decrease

Table 1: Proteins with increased abundance in lysates from SPOP pull down after radiation. Proteins were grouped based on changes in abundance in response to radiation as measured by mass spec analysis. This table shows proteins that were more abundant in SPOP pull down lysates following radiation.

Cell Cycle Proteins With Altered SPOP Interaction After Radiation	
Protein Name	Change
Bub3	Increase
Kif23	Increase
MST4	Increase
Rab GTPase-activating protein 1	Increase
CDK1	Decrease
MAPK	Decrease
Kinetochores Associated Protein 1	Decrease
R-ras2	Decrease
Regulator of chromosome condensation	Decrease
RhoA	Decrease
RuvB-like 1	Decrease
UHRF2	Decrease

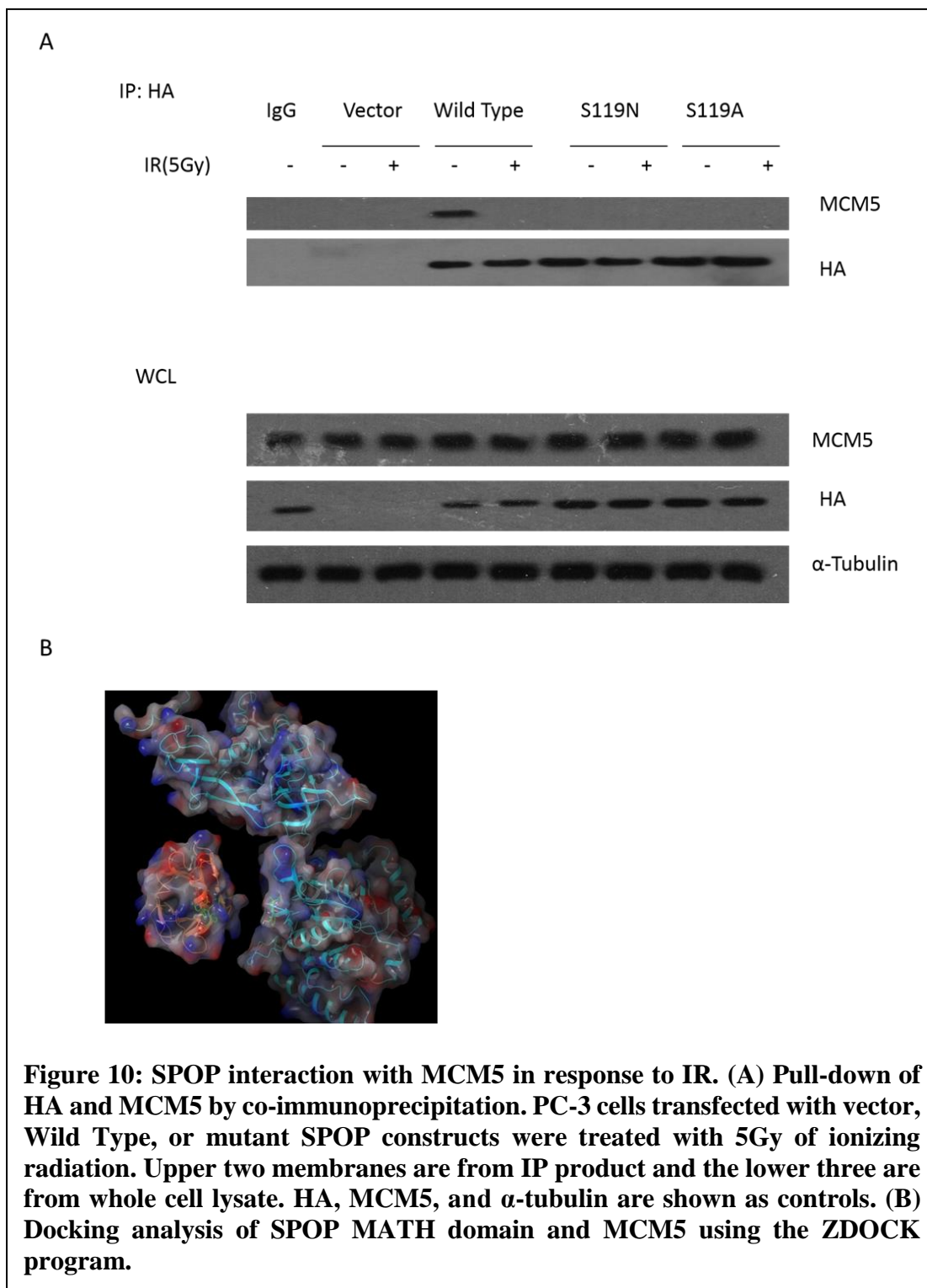
Table 2: Proteins with decreased abundance in lysates from SPOP pull down after radiation. Proteins were grouped based on changes in abundance in response to radiation as measured by mass spec analysis. This table shows proteins that were less abundant in SPOP pull down lysates following radiation.

With proteins that have a change in abundance based on their cell function of DDR and cell cycle control, we performed pathway analysis (www.string-db.org) based on the set of proteins that increased in abundance and the group that had decreased abundance. The major pathway for the proteins with increased SPOP interaction after IR is cell division (**Figure 9A**). This indicates that SPOP might target these proteins for destruction as a part of the DDR to prevent cell cycle progression. The major pathway for the set of proteins that had decreased expression after radiation is DNA duplex unwinding proteins (**Figure 9B**). This pathway suggests that SPOP dissociation with these proteins allow them to get access to DNA for appropriate damage sensing and repair.



SPOP interaction with MCM5 in response to IR

Due to the phenotypes we observed in S119/N-expressing cells (i.e. defects in G2/M checkpoint, and prolonged H2AX focus formation), we focused on validation of the interactions of SPOP with proteins that are significant to these processes. We selected Mini Chromosome Maintenance 5 (MCM5), a component of MCM helicase complex for validation (129-131). We found that in mock-treated cells, MCM5 was detectable in the HA precipitates. Consistent with the mass spectrometry data, MCM5 showed decreased interaction after IR (**Figure 10A**). These results demonstrate for that SPOP dissociated from MCM5 in response to DNA damage. Based on the recently reported MCM-5 structure (132), we found that MCM-5 (based on the X-ray structure of MCM complex, PDB ID: 3JA8) possesses a potential SBC (ITTTLN) motif in a fully exposed β -sheet conformation. The molecular surfaces and the electrostatic potential maps of the SPOP^{MATH} recruiting-motif (based on the X-ray structure of SPOP, PDB ID: 3HQI) (9) and the MCM-5 SBC-motif show good complementarity (**Figure 10B**). Docking studies using the ZDOCK (133) program resulted a well fitted MCM-5-SPOP^{MATH} complex model with the MCM-5 SBC-motif directly interacting with the recruiting residues of SPOP^{MATH} through both hydrophobic interactions and hydrogen bonds.



Discussion

Accumulating evidence support that, as a critical genome guardian mechanism, the DDR is a barrier to early tumorigenesis (1). As a crucial DDR pathway, ATM-mediated phosphorylation of downstream targets is essential for activation of cell cycle checkpoints, DNA repair and programmed cell death in the presence of DNA damage. However, it is rare that these phosphorylation sites show mutations in clinical samples, despite that germline and somatic mutations of DDR genes are frequently found. Here, we provide direct evidence that SPOP serine 119 connects to the ATM kinase, and that mutation of S119 leads to disruption of ATM-mediated DDR pathway and makes prostate cancer cells hypersensitive to IR treatment. These studies highlight pathophysiological evidence of a biochemical pathway to indicate a subset of patients with distinctive clinical responsiveness to radiotherapy.

Recent studies have indicated that SPOP plays a critical role in the DDR (71, 72). A clear mechanism driving this role remains to be fully understood. Of the mutations in the MATH domain we tested, only the S119N mutant showed significant hypersensitivity to IR, prompting us further investigate the potential role of the SPOP-ATM interaction. The biochemical connection of ATM and SPOP is highlighted in a series of experiments including *in situ* PLA, BLI and co-immunoprecipitation. Further experiments prove *in vitro* and in cell phosphorylation by the ATM kinase in response to DNA damage. The functional significance was demonstrated by the expression of mutant protein in prostate cancer cells and normal prostate epithelial cells. These results highlight a functionally important pathway that links ATM and its downstream targets of SPOP.

The mechanism of SPOP's involvement in the ATM-mediated DDR remains to be further investigated. It is possible that ATM and SPOP are brought together as a part of a larger complex. Previous studies showed that the other SPOP mutants also cause deficiencies in the DDR. This suggests that SPOP might have multiple roles or more residues in the MATH domain are needed for ATM interaction.

Additionally, the pathway downstream of SPOP in the context of DNA damage still remains to be further studied. The presence of DNA damage could change SPOP's affinity for different substrates. Since many of SPOP's confirmed substrates are oncogenic (25-27, 33, 117), a likely explanation is that SPOP downregulates those in order to help halt the cell cycle to give cells time to repair damaged DNA. Another possibility is that SPOP begins to interact with and ubiquitinate a new group of substrates to either tag them for degradation or to activate them. A third and potentially less likely scenario is that SPOP's role in the DDR is unrelated to its activity as an E3 adaptor protein and this new role is gated behind interaction with ATM. More investigation is needed to fully uncover this unexplored pathway in the DDR.

SILAC followed by mass spectrometry analysis provided two groups of proteins based on how their interaction with SPOP is changed by IR. Pathway analysis revealed that the set with increased interaction with SPOP contained proteins that are involved in cell division. This result is relatively expected, we hypothesize that upon radiation SPOP will target these proteins for degradation to halt the cell cycle. Conversely, proteins that dissociated with SPOP are involved in DNA unwinding, an essential aspect of DNA repair (134-137). We propose that dissociation increases availability allowing these proteins to then interact with DNA, resulting in unwinding. The unwound DNA can then be repaired.

Among the proteins interacting with SPOP identified by mass spectrometry, MCM5 is one protein that showed dissociation from SPOP in response to IR. Due to MCM5's critical role in DNA replication initiation and progress (138-140), it is likely that SPOP-MCM5 dissociation is a critical step for the cell cycle checkpoint and the maintenance of radiosensitivity.

Despite the unanswered questions of SPOP's role in the DDR, our data presented here holds clinical relevance for a sub group of individuals with prostate cancer. The evidence provided here suggests that patients with the SPOP S119N mutation might be more sensitive to radiation therapy. Radiation and other DNA damaging therapies such as chemotherapy are potentially more efficacious in this group.

SPOP REGULATION OF ITCH PROTECTS AGAINST PROSTATE CANCER
METASTASIS BY MAINTAINING E-CADHERIN

JINLU MA*, JOSHUA S. FRIED*, YUAN MA, CHENCHEN HE, MENGJIAO CAI,
LINYAN CHAI, SUXIA HAN, QINGHUA ZENG, AND BO XU

* Denotes co-first authors

In preparation for Endocrine-Related Cancer

Format adapted for Thesis

Abstract

Prostate cancer is one of the most common causes of cancer incidence and death in men, with late-stage and metastatic disease being the primary causes of mortality. SPOP is an E3 ubiquitin ligase adaptor protein that is often mutated in prostate cancer. In the present study, we use multivariate analysis to reveal that SPOP mutation correlates significantly with metastasis, independently of other clinical variables. We aimed to characterize a biochemical mechanism for the correlation between SPOP mutation and metastasis. Using proteomic analysis we identified candidate proteins for SPOP mediated degradation that also play a role in metastasis. Among the potential targets that fit this criteria was ITCH. We provide evidence that clinically relevant SPOP mutations disrupt the SPOP-ITCH interaction and lead to a subsequent increase in ITCH protein levels. We further demonstrate that SPOP mutation induced increases in ITCH protein levels lead to a concurrent loss of E-cadherin protein expression. Together, we analyzed a cohort of prostate cancer patients and observed that SPOP mutation correlated with metastasis. We then outline a SPOP-ITCH-E-cadherin pathway that impacts prostate cancer metastasis.

Key Words: SPOP, Prostate Cancer, ITCH, Metastasis

Introduction

Prostate cancer is currently among the leading causes of both cancer incidence and death in men (114). Mortality is largely due to advanced late stage and metastatic disease (141). There is a pressing need to better understand the underlying molecular drivers that render patients susceptible to more aggressive disease, so that they may be given appropriate and, subsequently, more potent therapies. Additionally, having the ability to identify which patients are less likely to develop aggressive disease can spare them from unnecessary treatments.

Prostate cancer is marked by several genetic aberrations. Most common among these alterations are ETS gene fusions, p53 aberrations, AR amplifications and SPOP missense mutations (115). SPOP is an E3 ubiquitin ligase adaptor that complexes with Cullin 3 to mediate the ubiquitination and destruction of target proteins (5, 9). Recent genetic studies of prostate cancer patients have identified the SPOP gene has the most common recurrent point mutations with 8-15% of the patient population carrying a somatic mutation (2, 18, 20, 21, 23, 142). Of these validated naturally occurring SPOP mutations, a significant number occur in the substrate binding MATH domain, suggesting physiological relevance. Tumor sequencing studies along with the database The Cancer Genome Atlas (TCGA) demonstrate SPOP mutation as an early event, and is exclusive with the common ETS gene fusion events in prostate cancer, making mutant SPOP tumors a distinct subgroup of prostate cancer (22). Many of SPOP's verified substrates are known oncoproteins such as SRC3, AR, and ERG. Due to SPOP's role in regulating drivers of oncogenesis it has emerged as potent tumor suppressor in prostate cancer and other cancers as well. Currently, there exists limited literature demonstrating the prognostic value of

SPOP expression level and mutational status, in depth studies are still needed to fully elucidate the clinical impact of SPOP as a diagnostic of prognostic tool.

The ITCH protein is an E3 ubiquitin ligase; ITCH mediated ubiquitination is integral in multiple cellular functions including the immune response, hematopoiesis, and lipid turnover (97, 143, 144). In the context of cancer, the ITCH function has shown to be both anti and pro tumorigenic. Studies show ITCH acts as a tumor suppressor by regulating HER and FLIP in breast and brain cancer respectively (102, 104-106, 108). Intriguingly, evidence also suggests ITCH can be a tumor promoter by down regulating Smad7, prompting TGF β to promote EMT, and inducing oncogenesis in breast cancer cells (112, 113). This suggest that ITCH's role in oncogenesis is subtype and / or context dependent.

In the present study, we first characterized a cohort of 198 prostate cancer patients. Multivariate analysis identified SPOP mutation as an independent predictor of metastasis in the patients. Proteomic analysis identified SPOP substrates that could be involved in metastasis. We then showed that SPOP, but not its mutants, binds to and regulates ITCH expression. Further, we demonstrate that SPOP mutants decrease the expression of E-cadherin. Together, we outline a SPOP ITCH E-cadherin signaling pathway that contributes to the prevention of prostate cancer metastasis.

Methods

Study population

Biopsies were obtained from 198 primary prostate tumors from patients (stage I-IV) at Cancer Center, the First Affiliated Hospital of Xi'an Jiaotong University from January 2010 to December 2015. In all cases, staging evaluation included a medical history and physical examination including a digital rectal examination, serum PSA (Prostate Serum Antigen), computed tomographic (CT) scan of the pelvis or an endorectal and pelvic coil magnetic resonance imaging (MRI) scan of the prostate and pelvis, bone scan, and a transrectal ultrasound-guided needle biopsy of the prostate with Gleason score histologic grading. The clinical stage was determined by the digital rectal examination findings using the 2002 American Joint Committee on Cancer (AJCC) staging system. Tumor size was defined as the maximum tumor diameter measured by pelvic coil MRI scan at the time of diagnosis. Follow-up data were available for all 198 patients; the median length of follow-up was 27 months (range 5 to 70 months). The study was approved by the Research and Ethical Committee of the First Affiliated Hospital of Xi'an Jiaotong University.

SPOP Mutation Analysis

DNA was extracted from frozen biopsy samples. 25-30mg of tissue were homogenized from each sample, DNA was extracted from the homogenate and quantified using Picogreen dsDNA Quantitation Reagent (Invitrogen, Carlsbad, CA, USA). Mutational analysis of SPOP was performed using a set of 4 primer pairs (**Table 1**) that covered the coding region of exons six and seven of the SPOP gene. All fragments were sequenced using the BigDye Terminator Cycle Sequencing Kit and ABI 3730 automated

sequencer (Applied Biosystems, Foster City, CA, USA). Each mutation was confirmed in duplicate testing.

Primer	Sequence
SPOP-6FO	5' AGGGAGATCGAGGTTGCA 3'
SPOP-6RO	5' TTTCTTGAATCCCCAGTCTTT 3' 571
SPOP-6F	5' TATGGGGCCTGCATTTGT 3'
SPOP-6R	5' CGCAAAAACCAGATCAAAGC 3' 349
SPOP-7FO	5' AAGAGTGAAGTTCGGGCAA 3'
SPOP-7RO	5' ACTGACACATACCAAGGTAGCATA 3' 568
SPOP-7F	5' TTAAGTTTCACATCCAGAAGTTTC 3'
SPOP-7R	5' GGGGCTTTTTCTTACTCTACATC 3' 327

Table 1: Primers used in sequencing. Forward and reverse primers used to sequence patient tumors to detect SPOP mutation(s).

Cell Culture

Human prostate cancer LNCaP cells (American Type Culture Collection) were cultured in DMEM medium (GIBCO-Invitrogen, Carlsbad, CA) containing 10% of FBS, 2mM of L-glutamine, 100 units/ml of penicillin, and 100mg/ml of streptomycin, and grown under standard cell culture conditions at 37°C in a humidified atmosphere with 5% CO₂.

SiRNA Depletion of SPOP

For RNAi experiments, ON-TARGET plus double-stranded siRNA oligomers against human SPOP and non-specific scrambled siRNA control (Stealth RNAi™ siRNA Negative Control, Med GC) were purchased from Thermo Scientific. Cells were transfected with Lipofectamine RNAiMAX (Invitrogen) with a final siRNA concentration of 50 nM according to the manufacturer's instructions.

Expression Constructs

Using Phusion High-Fidelity DNA Polymerase (New England BioLabs, Ipswich, MA, USA) and PCR primers containing an HA tag at the N terminus, an expression construct of HA-tagged SPOP (pcDNA3.1-HA-SPOP, wild-type) was constructed by insertion of the PCR-amplified SPOP cDNA-coding sequence into mammalian expression vector pcDNA3.1 Hygro (+) (Invitrogen). In vitro site-directed mutagenesis was used to obtain the HA-tagged SPOP mutants by two PCR amplifications using pcDNA3.1-HA-SPOP as the template. The PCR-amplified DNAs coding for mutated SPOPs were inserted into pcDNA3.1 Hygro (+) (Invitrogen) to generate the corresponding mammalian expression vectors: pcDNA3.1-HA-SPOPF133L, pcDNA3.1-HA-SPOPY87C, and pcDNA3.1-HA-SPOPW131G.

Western blotting

Cells in 6-well plates were lysed in 0.5 ml of lysis buffer (phosphate buffered saline containing 1% Triton X-100 and 1mM PMSF) at 4°C for 10 min. Equal quantities of protein were subjected to SDS-PAGE under reducing conditions. Following transfer to immobilon-Ptransfer membrane, successive incubations with a primary antibody, and a horseradish peroxidase-conjugated secondary antibody were carried out for 60–120 min at room temperature. The immunoreactive proteins were then detected using the ECL system. Films showing immunoreactive bands were scanned by Hp Scanjet 5590 (HP, Pal Alto, CA, USA). The antibodies used in Western blotting were mouse anti-HA (Roche, Basel, Switzerland), monoclonal mouse anti-FLAG M2 (Sigma, St. Louis, Mo, USA), anti-SPOP (Abcam, Cambridge, United Kingdom), monoclonal rabbit anti-ITCH (Cell Signaling, Danvers, MA, USA), rabbit anti-E-cadherin (Santa Cruz, Dallas, TX, USA), mouse anti-

FLAG-HRP (Sigma), mouse anti-HA-HRP (Roche), anti-rabbit IgG-HRP (Sigma), and anti-mouse IgG-HRP (Sigma).

Co-immunoprecipitation

Cell lysates were pre cleared for four hours with a matrix from Santa Cruz. After pre clearing antibody was added along with species specific beads (Santa Cruz). The lysates were rotated overnight in 4°C with the beads and antibody. The bead lysate mixture was washed once with PBS and spun down. The supernatant was then used for immunoblotting.

Statistical Analysis

The Fisher's exact tests were used to compare categorical data. The risk of metastasis among patients with SPOP mutation was evaluated using univariate and multivariate Cox regression analysis. Cox proportional hazards regression models were used to test the prognostic role of the SPOP mutation status (Hazard ratios [HR] and 95% confidence intervals [CI]). Two-sided P values less than 0.05 were considered to be statistically significant. All analyses were performed using the SPSS Statistics 20.0 software (Chicago, IL, USA).

Transwell Migration Assay

Well inserts (Corning, Corning, NY, USA) were coated with 100 µl of Matrigel (Corning) or serum free DMEM. 100,000 transfected PC-3 cells suspended in 200 µl of serum free DMEM were added to the inserts. 300 µl of complete media was added to the bottom of each well. 24 hours after plating the media was aspirated and Matrigel was removed with a sterile cotton swab. Inserts were washed with PBS and cells were then fixed in 2% paraformaldehyde for ten minutes. Following fixation cells were washed with

PBS and then stained with Hoechst 33342 (Invitrogen, Eugene, Oregon, USA). After staining the cells were once again washed with PBS and imaged with an EVOS fluorescent microscope (Life, Carlsbad, CA, USA). At least 3 different fields were captured for each sample, totaling over 30 cells. Invasion index was calculated by (number of cells in Matrigel / average number of cells in absence of Matrigel).

Results

Patient Characteristics

For the 198 patients, the age at diagnosis ranged from 44 to 91 years, with a median of 70 years. According to the AJCC staging system standards, 99 cases were stage I-II, 32 cases were stage III, and 67 cases were stage IV. 84% of patients had localized disease, and 15.1% had metastatic disease at diagnosis (**Table 2**).

Clinic Characteristic	Cases (N=198)	SPOP Mutation		P value
		Yes (N)	No (N)	
Age				0.82
≥ 75	61	6	55	
65-74	83	7	76	
55-64	45	3	42	
≤ 54	9	0	9	
Prior treatment PSA level				0.82
≤ 10	36	2	34	
10.1 - 20	39	3	36	
20.1 - 40	45	3	42	
≥ 40	78	8	70	
Gleason Score				0.17
≤ 6	50	3	47	
3+4/4+3	109	7	102	
≥ 8	39	6	33	
Stage				0.006
I-II	99	1	95	
III	32	5	25	
IV	67	10	61	
PSA Recurrence				0.008
Yes	26	6	20	
No	172	10	162	
Risk Group				0.02
Low	36	0	35	
Intermediate	108	5	102	
High	54	11	45	
Metastatic				0.00001
Yes	30	9	21	
No	168	7	161	

Table 2: Clinical characteristics of 198 patients with prostate cancer included in the study. Summary of the details of our patient cohort. Age, Prior PSA levels, Gleason Score, Stage, PSA recurrence, risk group and metastasis are displayed. Also the number of patients in each category are displayed along with SPOP mutation status. A p value comparing the presence or absence for SPOP mutation for each category is also displayed. From Dr. Jinlu Ma.

The frequency of SPOP mutations

To our knowledge there existed little data about the prevalence of SPOP mutation in Chinese men. To interrogate if SPOP mutation in this population is similar to that of western populations, we screened for somatic variants in exons six and seven, which code for the MATH domain, of the SPOP gene in 198 prostate tumor tissues. These two exons house the amino acids that have been previously reported as mutated in prostate cancer. Three somatic SPOP missense mutations were identified in 16 out of 198 tumor tissues (8%), and one somatic variant was identified in one tumor sample. The 16 patients who had SPOP mutations included mutations in the following codons (**Table 3**): phenylalanine (F) to valine (V) or leucine (L) or cysteine (C) substitution in codon 133 (F133V/L/C) (n = 7), tryptophan (W) to glycine (G) or cysteine (C) or serine (S) substitution in codon 131 (W131G/C/S) (n = 6), tyrosine (Y) to cysteine (C) or serine (S) substitution in codon 87 (Y87C/S) (n = 2), and phenylalanine (F) to leucine (L) (n = 1). The mutation rate of 8% is similar to the rate that has been reported in western populations; additionally the missense mutations we observed are also consistent with what has been reported previously.

AA CHANGE	N (%)
F133V/L/C	7 (43.8 %)
W131G/C/S	6 (37.5 %)
Y87C/S	2 (12.5 %)
F125L	1 (6.3 %)

Table 3: Localization and frequencies of SPOP mutations. Location, residue and frequency of the SPOP mutations identified in our cohort. From Dr. Jinlu Ma.

Correlation of SPOP Mutation with Metastasis

We also aimed to see if SPOP mutation correlated with other characteristics such as age and PSA level. Analysis of our cohort revealed that: patient's age, prior treatment PSA level and Gleason Score were not associated with SPOP mutation; however, mutation of SPOP was associated with risk and was significantly associated with metastasis (**Table 2**). SPOP mutant and wild-type tumors significantly differed in the pattern of metastatic involvement. SPOP mutant cases exhibited a higher incidence of metastasis compared with the wild-type cases. Metastases were located in the bone, liver, lung, and brain at the time of diagnosis in patients that had disseminated disease. Among patients with SPOP mutation, 56.3% showed metastasis at the time of diagnosis of primary cancer, compared to only 11.5% of patients with wild-type SPOP (OR, 6.58, 95% CI, 5.81-7.46, P = 0.000). The metastasis risk for patients with SPOP mutation was 1.27 times of the SPOP wild-type patients (OR, 1.27, 95% CI, 1.08-1.48, P = 0.003) (**Table 4**).

SPOP	Metastatic prostate cancer		Univariate analysis		Multivariate analysis	
	No. of Men (%)		OR	P	OR	P
	Yes (N=30)	No (N=168)	(95% CI)	value	(95% CI)	value
Mutated (N=16)	9 (56%)	7 (44%)	6.58 (5.81- 7.46)	0.000	1.27 (1.08- 1.48)	0.003
Wild- Type (N=182)	21 (11.5)	161 (88.5)				

Table 4: Associations between metastatic reporting at first diagnosis and SPOP mutations. Number of patients with metastatic disease as well as SPOP mutation status are displayed. Also univariate and multivariate analysis of the correlation between SPOP mutation status and metastatic disease are displayed. From Dr. Jinlu Ma.

Estimated prostate-specific antigen outcome for patients

We then wanted to determine if SPOP mutation had prognostic value in our patients. To this end we used biochemical relapse as measured by an increase in PSA levels. Of all 198 patients, 26 had evidence of biochemical relapse. The actuarial biochemical failure with SPOP mutation (**Figure 1A**) was 37.5% and 11.0% for patients with SPOP mutation and wild-type SPOP, respectively ($P < 0.0001$). The biochemical failure was 6.7% and 17.1% for patients with a PSA level of ≤ 20 and >20 ng/mL, respectively ($P = 0.0021$) (**Figure 1B**). We found no significant difference in the age groups (≤ 65 and > 65), as younger and older patients fared equally ($P = 0.527$) (**Figure 1C**). This data suggests that in our cohort SPOP did have strong prognostic value compared to age at diagnosis and PSA levels prior to treatment.

SPOP regulates ITCH protein expression

After the analysis revealed that SPOP mutation correlated strongly with metastasis, we sought to uncover a potential mechanism for this phenomenon. We performed proteomic analysis on lysates from prostate cancer cells in which SPOP was transiently knocked down by siRNA. Proteins that have altered expression upon the depletion of SPOP were identified. We then parsed our data by separating the proteins based on whether or not they had increased or decreased expression after SPOP knock down. Next, we focused upon proteins with increased abundance, as we hypothesized that these proteins could be potential SPOP substrates. This list was further analyzed by examining the amino acid sequences of the proteins and determining which have the characterized SPOP degron. From this list we then selected ITCH for validation and further experimentation as there exists evidence showing that it contributes to EMT.

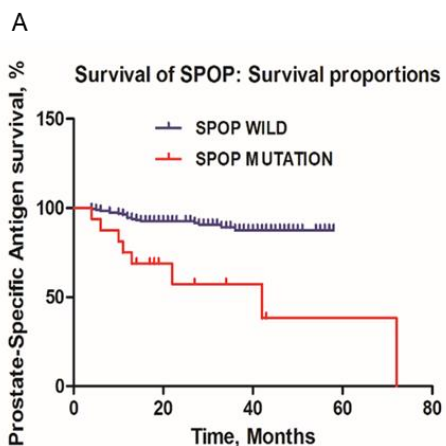
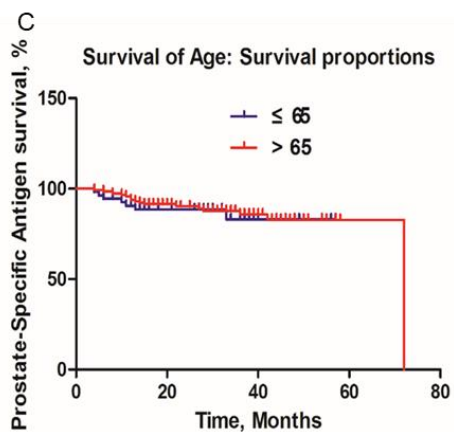
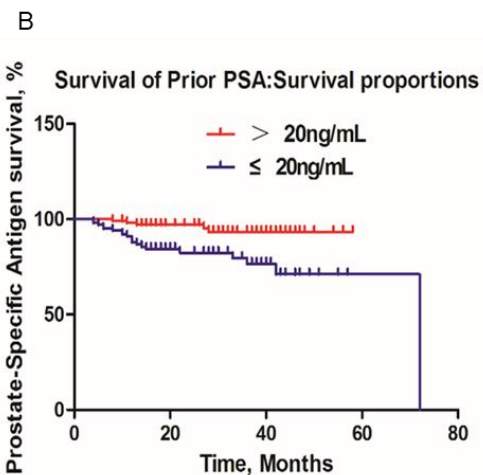
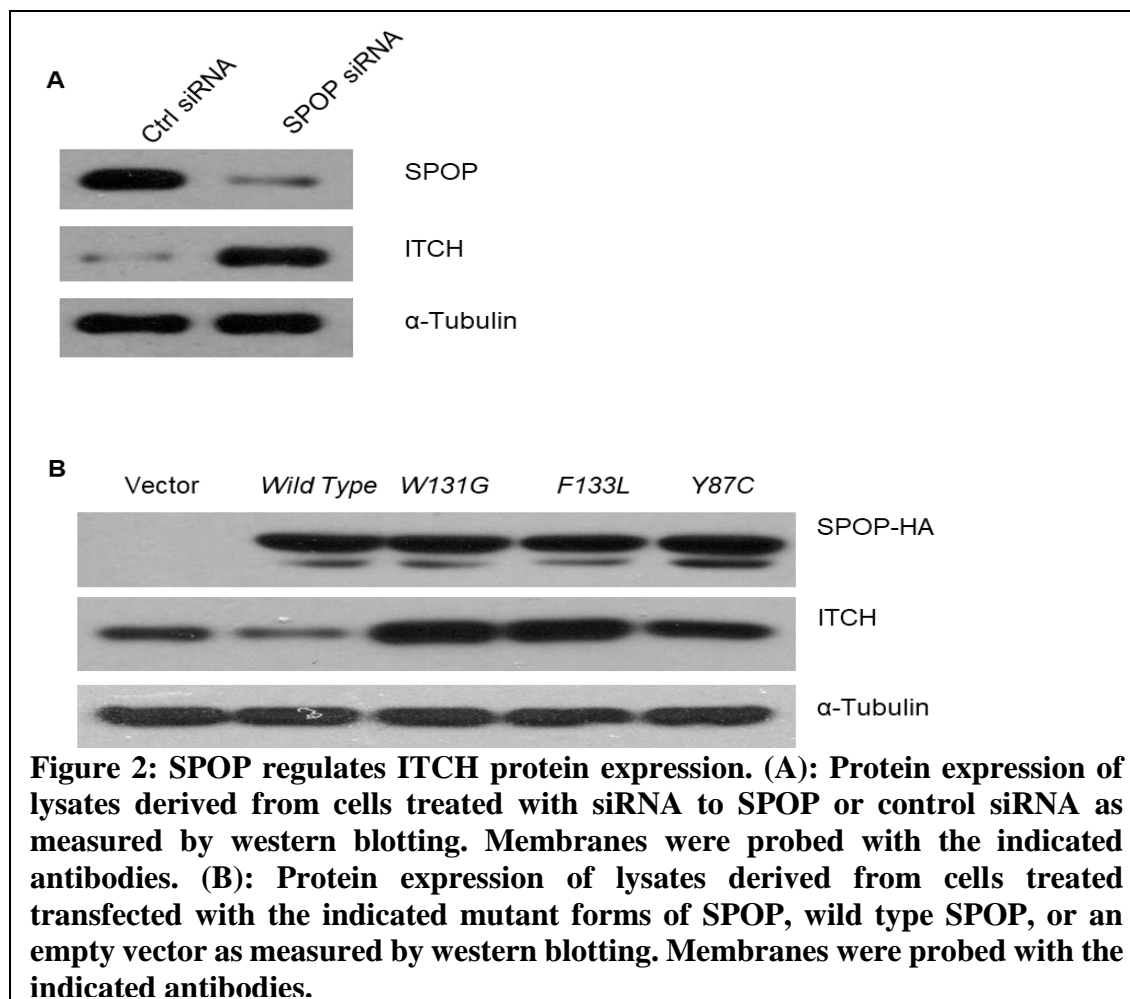


Figure 1: Actuarial analysis of all 198 patients for: (A) biochemical failure by SPOP mutation; (B) biochemical failure by Prior PSA level; (C) biochemical failure by age. All P values are from the log-rank test. From Dr. Jinlu Ma.

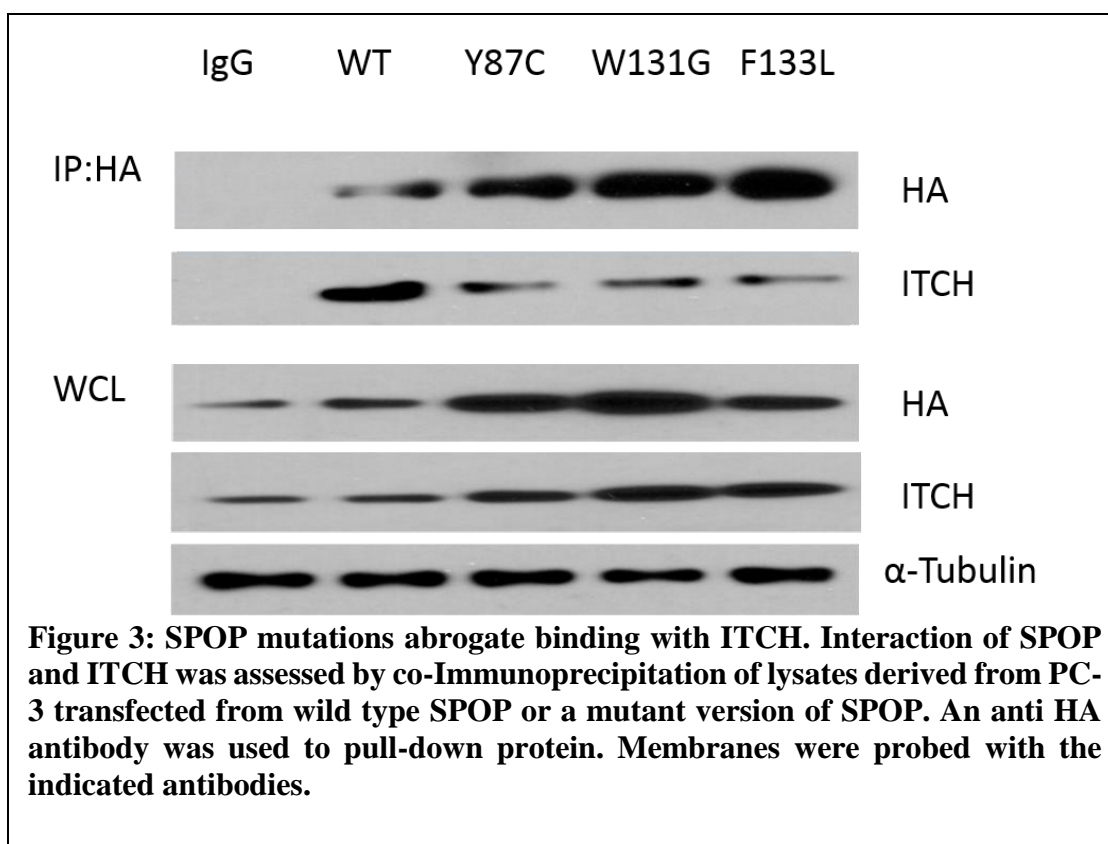


We began our validation by first using siRNA to deplete the expression of SPOP in prostate cancer cells and measuring the protein levels of ITCH via Western blot (**Figure 2A**). Knock down of SPOP caused a dramatic increase in ITCH protein accumulation that was not observed in cells treated with the control siRNA, indicating SPOP regulates ITCH protein turnover. We then tested if the clinically relevant SPOP mutations caused alteration on ITCH expression. We utilized the Y87C, W131G, and F133L mutations because these were present in our clinical cohort. All three of the investigated mutations caused an increase in ITCH protein, compared to wild type and vector transfected cells (**Figure 2B**). These results indicate that mutations of these MATH domain sites cause of loss of function of SPOP.



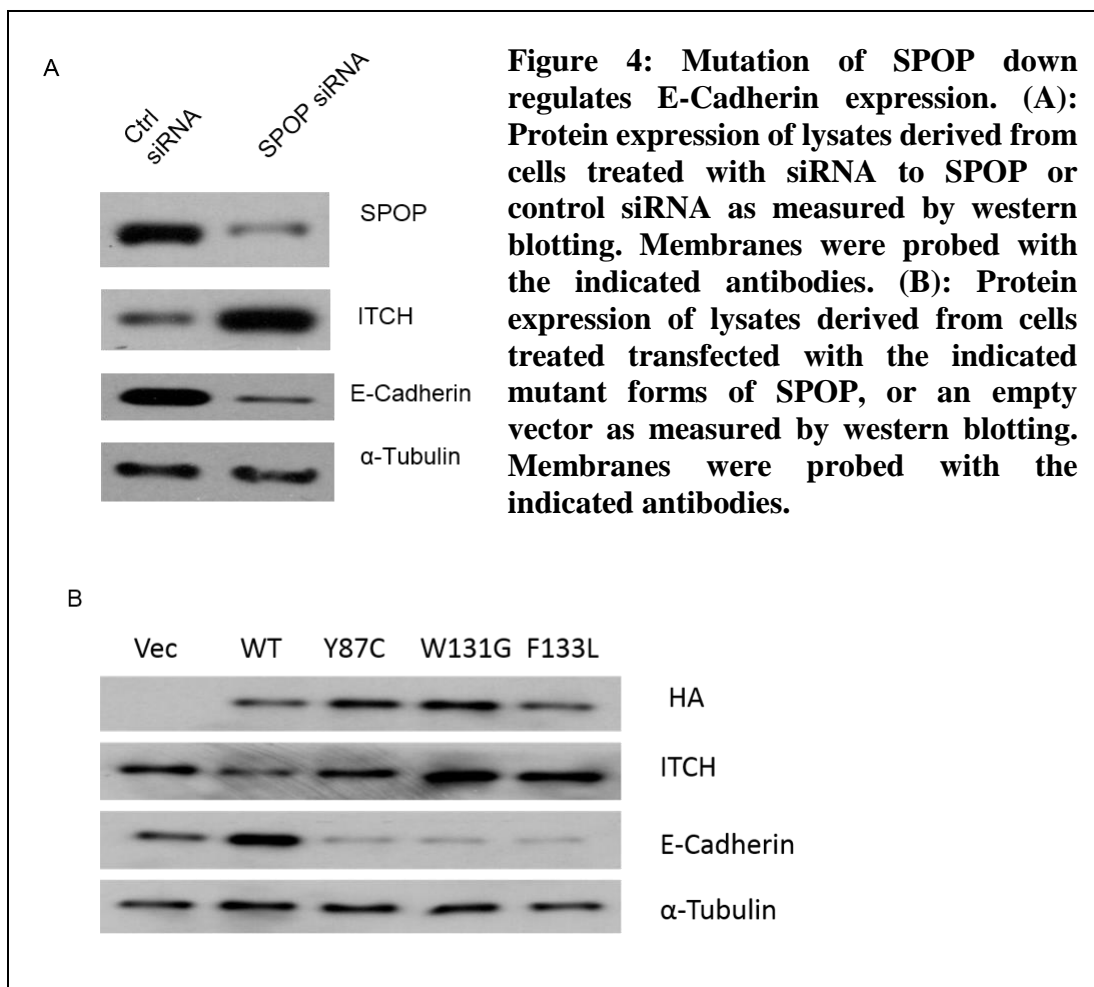
SPOP mutations abrogate binding with ITCH

Since ITCH protein levels were elevated in SPOP depleted cells, we determined that ITCH was a potential substrate of SPOP. To test this, we performed co-immunoprecipitation to determine if SPOP and ITCH interact and whether SPOP mutations alter the process. We then transfected prostate cancer cells with plasmids containing the mutant forms of SPOP. All three of the Y87C, W131G, and F133L mutant forms of SPOP abrogated SPOP-ITCH interaction as measured by co-immunoprecipitation (**Figure 3**). Taken together, ITCH interacts with SPOP and this interaction is ablated by SPOP mutation.



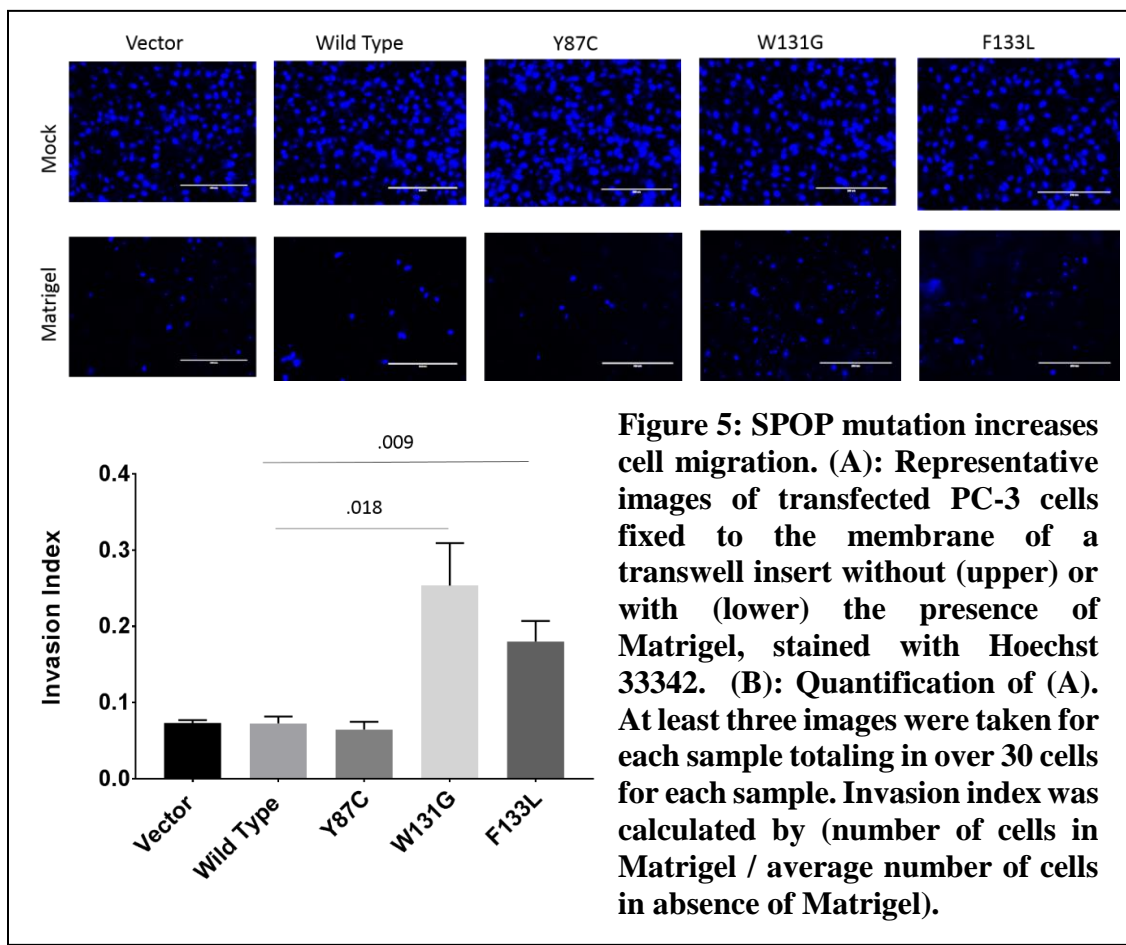
Mutation of SPOP down regulates E-Cadherin expression

To connect SPOP ITCH interaction and metastasis, we aimed to probe if E-Cadherin is impacted by the loss of this interaction. E-Cadherin is a tumor suppressor and known regulator of EMT (145-147). We began by investigating if SPOP depletion and subsequent ITCH induction changed E-cadherin protein levels. Cells with siRNA mediated knock down of SPOP had a marked reduction in E-cadherin levels with a concomitant rise in ITCH protein levels (**Figure 4A**). We next tested if SPOP mutation resulted in a similar phenotype as SPOP knock down. Expression of all three mutants caused a similar reduction in E-cadherin levels that was not observed in vector transfected cells (**Figure 4B**). In sum, loss of or mutation in SPOP causes a reduction in E-cadherin.



Mutation of SPOP promotes migration in vitro

We then sought to support our biochemical data with *in vitro* phenotypic assays. To this end we used the transwell migration assay to determine if mutation of SPOP could increase the migration capabilities of prostate cancer cells. Transfected PC-3 cells were plated into the inserts of transwells with or without the presence of Matrigel. 24 hours following plating the cells were fixed, stained and imaged. Two of the SPOP mutants, W131G, and F133L caused a significant increase in the fraction of cells that were able to migrate through the Matrigel (**Figure 5 A and B**). This data suggests that SPOP mutation can increase cell mobility and supports our clinical observations of SPOP mutation correlating with metastatic disease.



Discussion

In this study we began by analyzing the clinical characteristics of our patient cohort. Multivariate analysis revealed the presence of SPOP mutation as an independent predictor of prostate cancer metastasis. Using proteomic analysis and *in vitro* validation we identified ITCH as a novel SPOP substrate. With biochemical assays we observed that SPOP interacts with and regulates the expression of ITCH. The SPOP mutations present in our cohort interrupted the interaction and subsequently led to increased ITCH levels *in vitro*. We then demonstrated that SPOP regulation of ITCH is crucial to maintaining E-cadherin levels. Lastly, we provide *in vitro* evidence of SPOP mutation increasing cell migration. Together, our data shows a SPOP ITCH E-cadherin axis that protects against metastasis and when disturbed, contributes to the metastatic potential of prostate cancer.

Our observations are supported by previous reports that have indicated SPOP mutation increased the motility of prostate cancer cell *in vitro* and *in vivo* (24, 28). This cohort, while not ethnically diverse, exhibits a similar mutation rate and pattern to those seen in North American and European men indicating that mutation hot spots contained in exons 6 and 7 are not isolated to specific regional populations. To our knowledge we are the first to report SPOP having a strong correlation with metastasis and potential prognostic value. Although our evidence is contrary to existing literature, there is evidence suggesting that SPOP depletion does have a poor prognosis (19, 20, 148). A potential reason for our observation contrasting those that have been reported is the difference in the ethnicity of patient cohorts. The previously mentioned studies were conducted in men of largely Caucasian or African descent whereas our study was composed entirely of Chinese men.

The SPOP-ITCH interaction described here is one of many substrate enzyme interactions that affect disease progression in the context of SPOP mutation. This specific

interaction has a biochemical link to hallmark proteins differentially regulated during EMT. Additional studies will determine the weight of SPOP mediated ITCH in relation to other SPOP oncogenic substrates as the driver of metastasis.

Due to the frequency of SPOP mutational occurrence and the deadly nature of metastatic prostate cancer, our results have a clear clinical impact at least for this group of patients. In an era of medicine where tumors are being sequenced more frequently and personalized medicine is becoming more common, our observations have potential to influence physicians' treatment strategies. The data here suggests patients with mutated SPOP might have a significantly higher risk for advanced disease compared to others with wild type tumors and should be given more vigorous treatment regimens. It is also possible that our findings can be expanded to other cancers where SPOP is frequently mutated (endometrial, and thyroid) or lost (gastric, colon, among others).

DISCUSSION AND CONCLUSIONS

Mutations in the genome are often the cause of malignant disease; however, these mutations can also be utilized clinically in diagnosis, prognosis, and developing treatment strategies. SPOP is frequently mutated in prostate cancer and its impact on the course of the disease and treatment strategies are still being discovered. The work presented here highlights two effects of SPOP mutation on prostate cancer progression. Two distinct roles for SPOP are presented that show its impact on prostate cancer disease progression. One focuses on a non-canonical function of SPOP and its role in the DDR. The other demonstrates SPOP's canonical function as a tumor suppressor regulating protein levels of an oncogenic substrate. Its role in the DNA damage response emphasizes its ability to contribute to preventing prostate cancer formation. The evidence here showing that SPOP mutation could be correlated with metastatic disease shows that it also plays a critical role in impeding the progression of cancer. Both investigations show the profound impact protein mutation can have on disease progression. Combined, the data shown here demonstrates that a SPOP mutation can be especially deleterious because not only will the DDR be inhibited, but oncogenic substrates will become dysregulated. SPOP mutation can contribute to genome instability thereby potentially increasing the risk of aggressive disease.

Previous work has demonstrated that SPOP interacts with ATM in the context of DNA damage (71). The studies presented here have shown that SPOP serine 119 is

essential for this interaction. Additionally, the results indicate that SPOP is phosphorylated by ATM in the context of DNA damage. SPOP S119N interrupts this interaction and also causes increased radiosensitivity. Combined, these findings further support the hypothesis that SPOP is critically involved in the DDR. A proteomic screen was utilized to identify downstream targets of SPOP-ATM interaction in order to further delineate this pathway. Analysis revealed that multiple DDR and cell cycle proteins have differential interactions with SPOP in the context of DNA damage. We identified MCM5, a replication helicase, as a putative SPOP interacting protein. Interestingly, the data does not suggest that SPOP mediates MCM5 destruction. However, it does suggest that SPOP and MCM5 interact in some form in the unperturbed state, and that this interaction is lost upon DNA damage or SPOP mutation.

The observations reported here support existing literature demonstrating that SPOP has a function in the DDR. As part of its role in the DDR, we have identified SPOP as a novel substrate of ATM. It is possible that this activity is outside of the canonical function of SPOP as an E3 ligase adaptor protein. However, SPOP's role in the DDR could be based on its function of protein regulation, but only in the context of DNA damage. Additional studies focused on identifying downstream targets will clarify if SPOP has a function completely disparate from protein ubiquitination. This study underscores the importance of identifying and understanding non-canonical roles for SPOP activity outside of its role as a tumor suppressor, especially in prostate cancer, where there may be other functions outside of regulating oncoproteins.

When considering the data presented there are alternative interpretations and unanswered questions that remain for consideration. The main unanswered question is the

nature of SPOP-ATM interaction. The strength and duration of the interactions is greater than would be expected for a typical kinase substrate reaction (149). The observation of ATM pulling down with HA-SPOP via co-IP suggests there is something more than a simple phosphorylation event to this interaction. Additionally, the *in vitro* kinase data is the only data directly illustrating ATM phosphorylation of SPOP. However, the signal of p53 was far greater than that of SPOP. The strength and duration of the SPOP-ATM interaction could be contributing to this reduced phosphorylation signal due to the decreased turnover of substrate relative to p53. In order to better understand SPOP-ATM interaction one could investigate if other SPOP mutants interrupt this interaction. BLI data with the S119A mutant also showed reduced interaction with ATM (data not shown), suggesting the serine is crucial for interaction with ATM. Another line of experiments that could be done to gain further understanding of the importance of interaction of SPOP with ATM relative to phosphorylation is investigating the effects of a S119E mutant. Data that has not been included here shows that the glutamate substitution rescues the radiosensitive phenotype. However, interaction assays such as PLA, co-IP, and BLI would need to be performed with this mutant to determine if the phenotype can be rescued despite abrogation of ATM interaction. If so, this would indicate that that the physiological effect of the phosphorylation is what is crucial to genome stability and not simply interaction with ATM. Further, conducting the SILAC experiment with the S119E mutant and comparing the downstream interactions with wild type SPOP would illustrate which protein-protein interactions are reliant upon ATM binding more so phosphorylation of SPOP. It is possible that interaction with ATM changes SPOP's substrate pool. More proteomic screens in the

context of ATM interaction with SPOP would need to be performed in order to base this conclusion.

The physiological effect of SPOP-MCM5 interaction also has questions that remain to be answered. The first is the outcome of SPOP interaction with MCM5. The data presented in this work does not show that MCM5 levels are changed by interactions with SPOP, suggesting that it is not a substrate. Although, mutation in the MATH domain interrupted this interaction, indicating that MCM5 is a substrate of SPOP. The two proteins could be a part of a complex, but this seems unlikely as MCM5 is already a part of complex with other MCM family proteins involved in DNA replication. A potential outcome of SPOP-MCM5 interaction is that SPOP mono-ubiquitinates MCM5 in order to activate it. MCM5 would likely be less active after DNA damage because the DDR would prevent DNA replication, so the interaction with SPOP would not be needed. Another potential reason for DNA damage abrogating SPOP-MCM5 interaction is that ATM interaction and/or phosphorylation of SPOP S119 prevents MCM5 interaction. This then frees SPOP for participation in the DDR.

Future studies should focus on SPOP interaction with MCM5 and identifying other potential downstream proteins in order to target clinically exploitable regions of the protein. For example, mimetics can potentially be used to replace the lost MCM5 interaction upon mutation of SPOP. Additionally, this project will focus on the effects of SPOP S119N mutation on MCM5 activity. Specifically, it would be a worthy endeavor to investigate if MCM5 helicase activity or replication fork licensing function has been altered in the presence of DNA damage. The data presented herein demonstrates that mutation of SPOP S119 induces a radiosensitive phenotype. Additional *in vivo data* using

other DNA damaging agents and animal models will enable the project to move into the clinical setting. With enough clinical data support, we believe that the mutational status of this amino acid could be used to guide treatment regimens. Eventually, tumor sequencing can become part of a diagnostic panel as personalized medicine becomes standard in clinical care. Patients with SPOP S119N mutation could be directed toward DNA damage-inducing therapies such as ionizing radiation and certain chemotherapies. This guided approach could potentially spare this patient population from hormone therapy, which is currently frontline therapy for prostate cancer (150, 151). Clinical utilization of the knowledge gained from these experiments would be feasible, as no new therapies would be needed beyond sequencing a patient's tumor.

To this end, the clinical study presented involving a cohort of prostate cancer patients was analyzed for SPOP mutation status and disease outcome. Clinical analysis revealed that SPOP mutation correlated strongly with metastasis independent of other clinical variables such as age and prior PSA levels. We then sought to identify a novel SPOP substrate that could help explain the observed increase in metastasis. A proteomic screen was used to select for proteins with increased expression in the absence of SPOP that also contained the SPOP degron and had existing reports of involvement in metastasis or the EMT. ITCH was then selected for validation and further study. Biochemical analysis supported the screen and validated that ITCH protein levels increased upon SPOP depletion; further, ITCH protein accumulation was also increased in cells expressing mutant forms of SPOP that were present in the cohort. It was also observed that SPOP and ITCH interact, and that this interaction was lost when SPOP is mutated, suggesting that ITCH is a SPOP substrate in combination with the previous findings. Additionally,

biochemical data showed that SPOP mutation decreased E-cadherin levels concomitantly with increasing ITCH levels, supporting the clinical findings. Lastly, the biochemical data was supplemented with *in vitro* data showing that mutation of SPOP increased prostate cell migration.

To our knowledge, at the time of this writing, this study is the first of its kind investigating SPOP mutation in Chinese men. The clinical data revealed that the rate of SPOP mutation in this cohort was similar to the rates that have been reported in other ethnic populations. This demonstrates that SPOP mutation is a critical event in prostate cancer in multiple ethnic populations (Caucasian, African, and Chinese), comprising a significant portion of the male prostate cancer population. This suggests that future therapies aimed at these mutations and/or mutations in SPOP's MATH domain will also be efficacious in the Chinese male population. Larger studies will be needed to provide more conclusive results. The discovery of ITCH as a novel SPOP substrate adds it to the growing list of SPOP targets. These findings further support that SPOP, at least in prostate cancer, is a potent tumor suppressor with wide ranging influence of cellular signaling. This study provides clinically relevant evidence that SPOP-mediated ITCH accumulation can be targeted therapeutically, thereby overcoming the oncogenic accumulation of the protein that promotes EMT transition and metastasis.

Follow-up biochemical studies will aim to further elucidate the SPOP-ITCH pathway and reveal putative therapeutic targets. Additionally, the effects of SPOP mutation, and increased ITCH will be investigated with regards to canonical ITCH function. As stated previously, ITCH is involved in the immune response, functioning to keep the inflammatory response temporary (143). It is possible that increased ITCH due to

SPOP mutation could have an immune inhibiting effect, impeding the body's ability to mount an anti-tumor response. Upon validation by a larger cohort, this data will be able to guide treatment avenues based on the presence of SPOP mutation. Patients with mutant SPOP can immediately begin more aggressive therapies. The difference from our analysis showing SPOP mutant correlation with metastasis from other studies highlights the heterogeneity of disease, and differences among ethnic groups that must be considered when formulating clinical trials and creating treatment plans.

There are several remaining unanswered questions from this study that will need to be addressed in future investigations. For example, it will be important to determine the reasons the Y87C mutant did not increase invasiveness in cells despite having the same biochemical markers as the W131G and F133L mutants. This suggests that there are other pathways that Y87C has not affected, or that the dominant negative effect of this mutant was not as strong as the other two mutants in pathways that were not investigated in this study. However, the clinical data presented also did not show that every individual with a SPOP mutation also had metastatic disease, which indicates that there are other variables that have not yet been accounted for and will need to be investigated to understand the metastasis-promoting effect observed herein. Also, the connection between ITCH and E-cadherin remains unknown; specifically, whether the interaction is direct, or if there are intermediary steps. These questions can be answered by investigating if ITCH and E-cadherin interact directly via co-IP. Also, investigating if E-cadherin ubiquitination changes based on activity and / or protein levels of ITCH could help further define their interaction.

These studies demonstrate that the presence of SPOP mutation and alterations of specific residues can be used as deciding factors in creating treatment strategies to best reduce the burden of patients. The evidence presented here, combined with other studies in the field make it apparent that SPOP is a crucial tumor suppressor in the context of prostate cancer and will continue to be the subject of rigorous study in the future. Additionally, the understanding of SPOP function in an oncogenic environment will have a profound impact on prostate cancer treatment and prognosis going forward.

REFERENCES

1. Hanahan D, Weinberg RA. Hallmarks of cancer: the next generation. *Cell*. 2011;144(5):646-74.
2. Barbieri CE, Baca SC, Lawrence MS, Demichelis F, Blattner M, Theurillat JP, et al. Exome sequencing identifies recurrent SPOP, FOXA1 and MED12 mutations in prostate cancer. *Nature genetics*. 2012;44(6):685-9.
3. Bardwell VJ, Treisman R. The POZ domain: a conserved protein-protein interaction motif. *Genes & development*. 1994;8(14):1664-77.
4. Hernandez-Munoz I, Lund AH, van der Stoop P, Boutsma E, Muijrs I, Verhoeven E, et al. Stable X chromosome inactivation involves the PRC1 Polycomb complex and requires histone MACROH2A1 and the CULLIN3/SPOP ubiquitin E3 ligase. *Proceedings of the National Academy of Sciences of the United States of America*. 2005;102(21):7635-40.
5. Kwon JE, La M, Oh KH, Oh YM, Kim GR, Seol JH, et al. BTB domain-containing speckle-type POZ protein (SPOP) serves as an adaptor of Daxx for ubiquitination by Cul3-based ubiquitin ligase. *The Journal of biological chemistry*. 2006;281(18):12664-72.
6. Byun B, Tak H, Joe CO. BTB/POZ domain of speckle-type POZ protein (SPOP) confers proapoptotic function in HeLa cells. *BioFactors*. 2007;31(3-4):165-9.
7. Byun B, Jung Y. Repression of transcriptional activity of estrogen receptor alpha by a Cullin3/SPOP ubiquitin E3 ligase complex. *Molecules and cells*. 2008;25(2):289-93.

8. Li C, Ao J, Fu J, Lee DF, Xu J, Lonard D, et al. Tumor-suppressor role for the SPOP ubiquitin ligase in signal-dependent proteolysis of the oncogenic co-activator SRC-3/AIB1. *Oncogene*. 2011;30(42):4350-64.
9. Zhuang M, Calabrese MF, Liu J, Waddell MB, Nourse A, Hammel M, et al. Structures of SPOP-substrate complexes: insights into molecular architectures of BTB-Cul3 ubiquitin ligases. *Molecular cell*. 2009;36(1):39-50.
10. Takahashi I, Kameoka Y, Hashimoto K. MacroH2A1.2 binds the nuclear protein Spop. *Biochimica et biophysica acta*. 2002;1591(1-3):63-8.
11. Liu A, Desai BM, Stoffers DA. Identification of PCIF1, a POZ domain protein that inhibits PDX-1 (MODY4) transcriptional activity. *Molecular and cellular biology*. 2004;24(10):4372-83.
12. Choo KB, Chuang TJ, Lin WY, Chang CM, Tsai YH, Huang CJ. Evolutionary expansion of SPOP and associated TD/POZ gene family: impact of evolutionary route on gene expression pattern. *Gene*. 2010;460(1-2):39-47.
13. Hoeller D, Dikic I. Targeting the ubiquitin system in cancer therapy. *Nature*. 2009;458(7237):438-44.
14. Laney JD, Hochstrasser M. Analysis of protein ubiquitination. *Current protocols in protein science*. 2011;Chapter 14:Unit14 5.
15. Pintard L, Willems A, Peter M. Cullin-based ubiquitin ligases: Cul3-BTB complexes join the family. *The EMBO journal*. 2004;23(8):1681-7.
16. Stogios PJ, Downs GS, Jauhal JJ, Nandra SK, Prive GG. Sequence and structural analysis of BTB domain proteins. *Genome biology*. 2005;6(10):R82.

17. Nakayama KI, Nakayama K. Ubiquitin ligases: cell-cycle control and cancer. *Nature reviews Cancer*. 2006;6(5):369-81.
18. Haffner MC, Mosbrugger T, Esopi DM, Fedor H, Heaphy CM, Walker DA, et al. Tracking the clonal origin of lethal prostate cancer. *The Journal of clinical investigation*. 2013;123(11):4918-22.
19. Blattner M, Lee DJ, O'Reilly C, Park K, MacDonald TY, Khani F, et al. SPOP mutations in prostate cancer across demographically diverse patient cohorts. *Neoplasia*. 2014;16(1):14-20.
20. Khani F, Mosquera JM, Park K, Blattner M, O'Reilly C, MacDonald TY, et al. Evidence for molecular differences in prostate cancer between African American and Caucasian men. *Clinical cancer research : an official journal of the American Association for Cancer Research*. 2014;20(18):4925-34.
21. Jung SH, Shin S, Kim MS, Baek IP, Lee JY, Lee SH, et al. Genetic Progression of High Grade Prostatic Intraepithelial Neoplasia to Prostate Cancer. *European urology*. 2016;69(5):823-30.
22. Cancer Genome Atlas Research N. The Molecular Taxonomy of Primary Prostate Cancer. *Cell*. 2015;163(4):1011-25.
23. Vinceneux A, Bruyere F, Haillot O, Charles T, de la Taille A, Salomon L, et al. Ductal adenocarcinoma of the prostate: Clinical and biological profiles. *The Prostate*. 2017;77(12):1242-50.
24. Blattner M, Liu D, Robinson BD, Huang D, Poliakov A, Gao D, et al. SPOP Mutation Drives Prostate Tumorigenesis In Vivo through Coordinate Regulation of PI3K/mTOR and AR Signaling. *Cancer cell*. 2017;31(3):436-51.

25. Geng C, Kaochar S, Li M, Rajapakshe K, Fiskus W, Dong J, et al. SPOP regulates prostate epithelial cell proliferation and promotes ubiquitination and turnover of c-MYC oncoprotein. *Oncogene*. 2017;36(33):4767-77.
26. Geng C, He B, Xu L, Barbieri CE, Eedunuri VK, Chew SA, et al. Prostate cancer-associated mutations in speckle-type POZ protein (SPOP) regulate steroid receptor coactivator 3 protein turnover. *Proceedings of the National Academy of Sciences of the United States of America*. 2013;110(17):6997-7002.
27. An J, Wang C, Deng Y, Yu L, Huang H. Destruction of full-length androgen receptor by wild-type SPOP, but not prostate-cancer-associated mutants. *Cell reports*. 2014;6(4):657-69.
28. Geng C, Rajapakshe K, Shah SS, Shou J, Eedunuri VK, Foley C, et al. Androgen receptor is the key transcriptional mediator of the tumor suppressor SPOP in prostate cancer. *Cancer research*. 2014;74(19):5631-43.
29. Cai C, Balk SP. Intratumoral androgen biosynthesis in prostate cancer pathogenesis and response to therapy. *Endocrine-related cancer*. 2011;18(5):R175-82.
30. Ullman D, Dorn D, Rais-Bahrami S, Gordetsky J. Clinical Utility and Biologic Implications of Phosphatase and Tensin Homolog (PTEN) and ETS-related Gene (ERG) in Prostate Cancer. *Urology*. 2018;113:59-70.
31. Duan S, Pagano M. SPOP Mutations or ERG Rearrangements Result in Enhanced Levels of ERG to Promote Cell Invasion in Prostate Cancer. *Molecular cell*. 2015;59(6):883-4.
32. Huang Y, Tan N, Jia D, Jing Y, Wang Q, Li Z, et al. Speckle-type POZ protein is negatively associated with malignancies and inhibits cell proliferation and migration in

liver cancer. *Tumour biology : the journal of the International Society for Oncodevelopmental Biology and Medicine*. 2015;36(12):9753-61.

33. Gan W, Dai X, Lunardi A, Li Z, Inuzuka H, Liu P, et al. SPOP Promotes Ubiquitination and Degradation of the ERG Oncoprotein to Suppress Prostate Cancer Progression. *Molecular cell*. 2015;59(6):917-30.

34. Theurillat JP, Udeshi ND, Errington WJ, Svinkina T, Baca SC, Pop M, et al. Prostate cancer. Ubiquitylome analysis identifies dysregulation of effector substrates in SPOP-mutant prostate cancer. *Science*. 2014;346(6205):85-9.

35. Wu F, Dai X, Gan W, Wan L, Li M, Mitsiades N, et al. Prostate cancer-associated mutation in SPOP impairs its ability to target Cdc20 for poly-ubiquitination and degradation. *Cancer letters*. 2017;385:207-14.

36. Groner AC, Cato L, de Tribolet-Hardy J, Bernasocchi T, Janouskova H, Melchers D, et al. TRIM24 Is an Oncogenic Transcriptional Activator in Prostate Cancer. *Cancer cell*. 2016;29(6):846-58.

37. Zhang L, Peng S, Dai X, Gan W, Nie X, Wei W, et al. Tumor suppressor SPOP ubiquitinates and degrades EglN2 to compromise growth of prostate cancer cells. *Cancer letters*. 2017;390:11-20.

38. Jin X, Wang J, Gao K, Zhang P, Yao L, Tang Y, et al. Dysregulation of INF2-mediated mitochondrial fission in SPOP-mutated prostate cancer. *PLoS genetics*. 2017;13(4):e1006748.

39. Zhu H, Ren S, Bitler BG, Aird KM, Tu Z, Skordalakes E, et al. SPOP E3 Ubiquitin Ligase Adaptor Promotes Cellular Senescence by Degrading the SENP7 deSUMOylase. *Cell reports*. 2015;13(6):1183-93.

40. Zhang P, Gao K, Tang Y, Jin X, An J, Yu H, et al. Destruction of DDIT3/CHOP protein by wild-type SPOP but not prostate cancer-associated mutants. *Human mutation*. 2014;35(9):1142-51.
41. Zhu K, Lei PJ, Ju LG, Wang X, Huang K, Yang B, et al. SPOP-containing complex regulates SETD2 stability and H3K36me3-coupled alternative splicing. *Nucleic acids research*. 2017;45(1):92-105.
42. Hoeijmakers JH. DNA damage, aging, and cancer. *The New England journal of medicine*. 2009;361(15):1475-85.
43. Alt FW, Zhang Y, Meng FL, Guo C, Schwer B. Mechanisms of programmed DNA lesions and genomic instability in the immune system. *Cell*. 2013;152(3):417-29.
44. Jackson SP, Bartek J. The DNA-damage response in human biology and disease. *Nature*. 2009;461(7267):1071-8.
45. Ciccio A, Elledge SJ. The DNA damage response: making it safe to play with knives. *Molecular cell*. 2010;40(2):179-204.
46. Jiricny J. The multifaceted mismatch-repair system. *Nature reviews Molecular cell biology*. 2006;7(5):335-46.
47. Lindahl T, Barnes DE. Repair of endogenous DNA damage. *Cold Spring Harbor symposia on quantitative biology*. 2000;65:127-33.
48. Moldovan GL, D'Andrea AD. How the fanconi anemia pathway guards the genome. *Annual review of genetics*. 2009;43:223-49.
49. Caldecott KW. Single-strand break repair and genetic disease. *Nature reviews Genetics*. 2008;9(8):619-31.

50. West SC. Molecular views of recombination proteins and their control. *Nature reviews Molecular cell biology*. 2003;4(6):435-45.
51. Zhou BB, Elledge SJ. The DNA damage response: putting checkpoints in perspective. *Nature*. 2000;408(6811):433-9.
52. Harper JW, Elledge SJ. The DNA damage response: ten years after. *Molecular cell*. 2007;28(5):739-45.
53. Taylor AM, Lam Z, Last JI, Byrd PJ. Ataxia telangiectasia: more variation at clinical and cellular levels. *Clinical genetics*. 2015;87(3):199-208.
54. Gotoff SP, Amirmokri E, Liebner EJ. Ataxia telangiectasia. Neoplasia, untoward response to x-irradiation, and tuberous sclerosis. *American journal of diseases of children*. 1967;114(6):617-25.
55. Taylor AM, Harnden DG, Arlett CF, Harcourt SA, Lehmann AR, Stevens S, et al. Ataxia telangiectasia: a human mutation with abnormal radiation sensitivity. *Nature*. 1975;258(5534):427-9.
56. Imray FP, Kidson C. Perturbations of cell-cycle progression in gamma-irradiated ataxia telangiectasia and Huntington's disease cells detected by DNA flow cytometric analysis. *Mutation research*. 1983;112(6):369-82.
57. Nagasawa H, Little JB. Comparison of kinetics of X-ray-induced cell killing in normal, ataxia telangiectasia and hereditary retinoblastoma fibroblasts. *Mutation research*. 1983;109(2):297-308.
58. Zampetti-Bosseler F, Scott D. Cell death, chromosome damage and mitotic delay in normal human, ataxia telangiectasia and retinoblastoma fibroblasts after x-irradiation.

International journal of radiation biology and related studies in physics, chemistry, and medicine. 1981;39(5):547-58.

59. Biton S, Barzilai A, Shiloh Y. The neurological phenotype of ataxia-telangiectasia: solving a persistent puzzle. *DNA repair*. 2008;7(7):1028-38.

60. Bosotti R, Isacchi A, Sonnhammer EL. FAT: a novel domain in PIK-related kinases. *Trends in biochemical sciences*. 2000;25(5):225-7.

61. Mordes DA, Glick GG, Zhao R, Cortez D. TopBP1 activates ATR through ATRIP and a PIKK regulatory domain. *Genes & development*. 2008;22(11):1478-89.

62. Falck J, Coates J, Jackson SP. Conserved modes of recruitment of ATM, ATR and DNA-PKcs to sites of DNA damage. *Nature*. 2005;434(7033):605-11.

63. Bakkenist CJ, Kastan MB. DNA damage activates ATM through intermolecular autophosphorylation and dimer dissociation. *Nature*. 2003;421(6922):499-506.

64. Kim ST, Lim DS, Canman CE, Kastan MB. Substrate specificities and identification of putative substrates of ATM kinase family members. *The Journal of biological chemistry*. 1999;274(53):37538-43.

65. Rogakou EP, Pilch DR, Orr AH, Ivanova VS, Bonner WM. DNA double-stranded breaks induce histone H2AX phosphorylation on serine 139. *The Journal of biological chemistry*. 1998;273(10):5858-68.

66. Haince JF, Kozlov S, Dawson VL, Dawson TM, Hendzel MJ, Lavin MF, et al. Ataxia telangiectasia mutated (ATM) signaling network is modulated by a novel poly(ADP-ribose)-dependent pathway in the early response to DNA-damaging agents. *The Journal of biological chemistry*. 2007;282(22):16441-53.

67. Hirao A, Cheung A, Duncan G, Girard PM, Elia AJ, Wakeham A, et al. Chk2 is a tumor suppressor that regulates apoptosis in both an ataxia telangiectasia mutated (ATM)-dependent and an ATM-independent manner. *Molecular and cellular biology*. 2002;22(18):6521-32.
68. Jack MT, Woo RA, Hirao A, Cheung A, Mak TW, Lee PW. Chk2 is dispensable for p53-mediated G1 arrest but is required for a latent p53-mediated apoptotic response. *Proceedings of the National Academy of Sciences of the United States of America*. 2002;99(15):9825-9.
69. Takai H, Naka K, Okada Y, Watanabe M, Harada N, Saito S, et al. Chk2-deficient mice exhibit radioresistance and defective p53-mediated transcription. *The EMBO journal*. 2002;21(19):5195-205.
70. Shiloh Y, Ziv Y. The ATM protein kinase: regulating the cellular response to genotoxic stress, and more. *Nature reviews Molecular cell biology*. 2013;14(4):197-210.
71. Zhang D, Wang H, Sun M, Yang J, Zhang W, Han S, et al. Speckle-type POZ protein, SPOP, is involved in the DNA damage response. *Carcinogenesis*. 2014;35(8):1691-7.
72. Boysen G, Barbieri CE, Prandi D, Blattner M, Chae SS, Dahija A, et al. SPOP mutation leads to genomic instability in prostate cancer. *eLife*. 2015;4.
73. Matt S, Hofmann TG. The DNA damage-induced cell death response: a roadmap to kill cancer cells. *Cellular and molecular life sciences : CMLS*. 2016;73(15):2829-50.
74. Kalluri R, Weinberg RA. The basics of epithelial-mesenchymal transition. *The Journal of clinical investigation*. 2009;119(6):1420-8.

75. Nieto MA, Huang RY, Jackson RA, Thiery JP. Emt: 2016. *Cell*. 2016;166(1):21-45.
76. Thiery JP. Epithelial-mesenchymal transitions in tumour progression. *Nature reviews Cancer*. 2002;2(6):442-54.
77. Polyak K, Weinberg RA. Transitions between epithelial and mesenchymal states: acquisition of malignant and stem cell traits. *Nature reviews Cancer*. 2009;9(4):265-73.
78. De Craene B, Berx G. Regulatory networks defining EMT during cancer initiation and progression. *Nature reviews Cancer*. 2013;13(2):97-110.
79. Lamouille S, Xu J, Derynck R. Molecular mechanisms of epithelial-mesenchymal transition. *Nature reviews Molecular cell biology*. 2014;15(3):178-96.
80. Kourtidis A, Lu R, Pence LJ, Anastasiadis PZ. A central role for cadherin signaling in cancer. *Experimental cell research*. 2017;358(1):78-85.
81. Rasheed ZA, Yang J, Wang Q, Kowalski J, Freed I, Murter C, et al. Prognostic significance of tumorigenic cells with mesenchymal features in pancreatic adenocarcinoma. *Journal of the National Cancer Institute*. 2010;102(5):340-51.
82. Kong D, Banerjee S, Ahmad A, Li Y, Wang Z, Sethi S, et al. Epithelial to mesenchymal transition is mechanistically linked with stem cell signatures in prostate cancer cells. *PloS one*. 2010;5(8):e12445.
83. Fan F, Samuel S, Evans KW, Lu J, Xia L, Zhou Y, et al. Overexpression of snail induces epithelial-mesenchymal transition and a cancer stem cell-like phenotype in human colorectal cancer cells. *Cancer medicine*. 2012;1(1):5-16.

84. Long H, Xiang T, Qi W, Huang J, Chen J, He L, et al. CD133+ ovarian cancer stem-like cells promote non-stem cancer cell metastasis via CCL5 induced epithelial-mesenchymal transition. *Oncotarget*. 2015;6(8):5846-59.
85. Pastushenko I, Brisebarre A, Sifrim A, Fioramonti M, Revenco T, Boumahdi S, et al. Identification of the tumour transition states occurring during EMT. *Nature*. 2018;556(7702):463-8.
86. Shibue T, Weinberg RA. EMT, CSCs, and drug resistance: the mechanistic link and clinical implications. *Nature reviews Clinical oncology*. 2017;14(10):611-29.
87. Thiery JP, Acloque H, Huang RY, Nieto MA. Epithelial-mesenchymal transitions in development and disease. *Cell*. 2009;139(5):871-90.
88. Lambert AW, Pattabiraman DR, Weinberg RA. Emerging Biological Principles of Metastasis. *Cell*. 2017;168(4):670-91.
89. Fidler IJ. The pathogenesis of cancer metastasis: the 'seed and soil' hypothesis revisited. *Nature reviews Cancer*. 2003;3(6):453-8.
90. Gupta GP, Massague J. Cancer metastasis: building a framework. *Cell*. 2006;127(4):679-95.
91. Talmadge JE, Fidler IJ. AACR centennial series: the biology of cancer metastasis: historical perspective. *Cancer research*. 2010;70(14):5649-69.
92. Marchese A, Raiborg C, Santini F, Keen JH, Stenmark H, Benovic JL. The E3 ubiquitin ligase AIP4 mediates ubiquitination and sorting of the G protein-coupled receptor CXCR4. *Developmental cell*. 2003;5(5):709-22.

93. Yang C, Zhou W, Jeon MS, Demydenko D, Harada Y, Zhou H, et al. Negative regulation of the E3 ubiquitin ligase itch via Fyn-mediated tyrosine phosphorylation. *Molecular cell*. 2006;21(1):135-41.
94. Scialpi F, Malatesta M, Peschiaroli A, Rossi M, Melino G, Bernassola F. Itch self-polyubiquitylation occurs through lysine-63 linkages. *Biochemical pharmacology*. 2008;76(11):1515-21.
95. Hooper C, Puttamadappa SS, Loring Z, Shekhtman A, Bakowska JC. Spartin activates atrophin-1-interacting protein 4 (AIP4) E3 ubiquitin ligase and promotes ubiquitination of adipophilin on lipid droplets. *BMC biology*. 2010;8:72.
96. Edwards TL, Clowes VE, Tsang HT, Connell JW, Sanderson CM, Luzio JP, et al. Endogenous spartin (SPG20) is recruited to endosomes and lipid droplets and interacts with the ubiquitin E3 ligases AIP4 and AIP5. *The Biochemical journal*. 2009;423(1):31-9.
97. Alberts P, Rotin D. Regulation of lipid droplet turnover by ubiquitin ligases. *BMC biology*. 2010;8:94.
98. Milewska M, McRedmond J, Byrne PC. Identification of novel spartin-interactors shows spartin is a multifunctional protein. *Journal of neurochemistry*. 2009;111(4):1022-30.
99. Vartanian R, Masri J, Martin J, Cloninger C, Holmes B, Artinian N, et al. AP-1 regulates cyclin D1 and c-MYC transcription in an AKT-dependent manner in response to mTOR inhibition: role of AIP4/Itch-mediated JUNB degradation. *Molecular cancer research : MCR*. 2011;9(1):115-30.

100. Fang D, Kerppola TK. Ubiquitin-mediated fluorescence complementation reveals that Jun ubiquitinated by Itch/AIP4 is localized to lysosomes. *Proceedings of the National Academy of Sciences of the United States of America*. 2004;101(41):14782-7.
101. Anzi S, Finkin S, Shaulian E. Transcriptional repression of c-Jun's E3 ubiquitin ligases contributes to c-Jun induction by UV. *Cellular signalling*. 2008;20(5):862-71.
102. Panner A, Crane CA, Weng C, Feletti A, Fang S, Parsa AT, et al. Ubiquitin-specific protease 8 links the PTEN-Akt-AIP4 pathway to the control of FLIPS stability and TRAIL sensitivity in glioblastoma multiforme. *Cancer research*. 2010;70(12):5046-53.
103. Yerbes R, Lopez-Rivas A. Itch/AIP4-independent proteasomal degradation of cFLIP induced by the histone deacetylase inhibitor SAHA sensitizes breast tumour cells to TRAIL. *Investigational new drugs*. 2012;30(2):541-7.
104. Panner A, Crane CA, Weng C, Feletti A, Parsa AT, Pieper RO. A novel PTEN-dependent link to ubiquitination controls FLIPS stability and TRAIL sensitivity in glioblastoma multiforme. *Cancer research*. 2009;69(20):7911-6.
105. Le Cloennec C, Lazrek Y, Dubreuil O, Larbouret C, Poul MA, Mondon P, et al. The anti-HER3 (ErbB3) therapeutic antibody 9F7-F11 induces HER3 ubiquitination and degradation in tumors through JNK1/2- dependent ITCH/AIP4 activation. *Oncotarget*. 2016;7(24):37013-29.
106. Omerovic J, Santangelo L, Puggioni EM, Marrocco J, Dall'Armi C, Palumbo C, et al. The E3 ligase Aip4/Itch ubiquitinates and targets ErbB-4 for degradation. *FASEB journal : official publication of the Federation of American Societies for Experimental Biology*. 2007;21(11):2849-62.

107. Courbard JR, Fiore F, Adelaide J, Borg JP, Birnbaum D, Ollendorff V. Interaction between two ubiquitin-protein isopeptide ligases of different classes, CBLC and AIP4/ITCH. *The Journal of biological chemistry*. 2002;277(47):45267-75.
108. Li Y, Zhou Z, Alimandi M, Chen C. WW domain containing E3 ubiquitin protein ligase 1 targets the full-length ErbB4 for ubiquitin-mediated degradation in breast cancer. *Oncogene*. 2009;28(33):2948-58.
109. Demange C, Ferrand N, Prunier C, Bourgeade MF, Atfi A. A model of partnership co-opted by the homeodomain protein TGIF and the Itch/AIP4 ubiquitin ligase for effective execution of TNF-alpha cytotoxicity. *Molecular cell*. 2009;36(6):1073-85.
110. Lallemand F, Seo SR, Ferrand N, Pessah M, L'Hoste S, Rawadi G, et al. AIP4 restricts transforming growth factor-beta signaling through a ubiquitination-independent mechanism. *The Journal of biological chemistry*. 2005;280(30):27645-53.
111. Feng L, Guedes S, Wang T. Atrophin-1-interacting protein 4/human Itch is a ubiquitin E3 ligase for human enhancer of filamentation 1 in transforming growth factor-beta signaling pathways. *The Journal of biological chemistry*. 2004;279(28):29681-90.
112. Park SH, Jung EH, Kim GY, Kim BC, Lim JH, Woo CH. Itch E3 ubiquitin ligase positively regulates TGF-beta signaling to EMT via Smad7 ubiquitination. *Molecules and cells*. 2015;38(1):20-5.
113. Salah Z, Itzhaki E, Aqeilan RI. The ubiquitin E3 ligase ITCH enhances breast tumor progression by inhibiting the Hippo tumor suppressor pathway. *Oncotarget*. 2014;5(21):10886-900.
114. Siegel RL, Miller KD, Jemal A. *Cancer Statistics, 2017*. CA: a cancer journal for clinicians. 2017;67(1):7-30.

115. Grasso CS, Wu YM, Robinson DR, Cao X, Dhanasekaran SM, Khan AP, et al. The mutational landscape of lethal castration-resistant prostate cancer. *Nature*. 2012;487(7406):239-43.
116. Tomlins SA, Laxman B, Dhanasekaran SM, Helgeson BE, Cao X, Morris DS, et al. Distinct classes of chromosomal rearrangements create oncogenic ETS gene fusions in prostate cancer. *Nature*. 2007;448(7153):595-9.
117. Dai X, Gan W, Li X, Wang S, Zhang W, Huang L, et al. Prostate cancer-associated SPOP mutations confer resistance to BET inhibitors through stabilization of BRD4. *Nature medicine*. 2017;23(9):1063-71.
118. Taylor AM, Metcalfe JA, Oxford JM, Harnden DG. Is chromatid-type damage in ataxia telangiectasia after irradiation at G0 a consequence of defective repair? *Nature*. 1976;260(5550):441-3.
119. Kang J, Ferguson D, Song H, Bassing C, Eckersdorff M, Alt FW, et al. Functional interaction of H2AX, NBS1, and p53 in ATM-dependent DNA damage responses and tumor suppression. *Molecular and cellular biology*. 2005;25(2):661-70.
120. Savic V, Yin B, Maas NL, Bredemeyer AL, Carpenter AC, Helmink BA, et al. Formation of dynamic gamma-H2AX domains along broken DNA strands is distinctly regulated by ATM and MDC1 and dependent upon H2AX densities in chromatin. *Molecular cell*. 2009;34(3):298-310.
121. Burma S, Chen BP, Murphy M, Kurimasa A, Chen DJ. ATM phosphorylates histone H2AX in response to DNA double-strand breaks. *The Journal of biological chemistry*. 2001;276(45):42462-7.

122. Elledge SJ. Cell cycle checkpoints: preventing an identity crisis. *Science*. 1996;274(5293):1664-72.
123. Weinert TA, Hartwell LH. The RAD9 gene controls the cell cycle response to DNA damage in *Saccharomyces cerevisiae*. *Science*. 1988;241(4863):317-22.
124. Serrano D, D'Amours D. When genome integrity and cell cycle decisions collide: roles of polo kinases in cellular adaptation to DNA damage. *Systems and synthetic biology*. 2014;8(3):195-203.
125. Hoffelder DR, Luo L, Burke NA, Watkins SC, Gollin SM, Saunders WS. Resolution of anaphase bridges in cancer cells. *Chromosoma*. 2004;112(8):389-97.
126. Terradas M, Martin M, Tusell L, Genesca A. Genetic activities in micronuclei: is the DNA entrapped in micronuclei lost for the cell? *Mutation research*. 2010;705(1):60-7.
127. Shah NB, Duncan TM. Bio-layer interferometry for measuring kinetics of protein-protein interactions and allosteric ligand effects. *Journal of visualized experiments : JoVE*. 2014(84):e51383.
128. Matsuoka S, Ballif BA, Smogorzewska A, McDonald ER, 3rd, Hurov KE, Luo J, et al. ATM and ATR substrate analysis reveals extensive protein networks responsive to DNA damage. *Science*. 2007;316(5828):1160-6.
129. Bochman ML, Schwacha A. The Mcm complex: unwinding the mechanism of a replicative helicase. *Microbiology and molecular biology reviews : MMBR*. 2009;73(4):652-83.
130. Erzberger JP, Berger JM. Evolutionary relationships and structural mechanisms of AAA+ proteins. *Annual review of biophysics and biomolecular structure*. 2006;35:93-114.


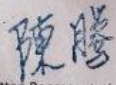
131. Iyer LM, Leipe DD, Koonin EV, Aravind L. Evolutionary history and higher order classification of AAA+ ATPases. *Journal of structural biology*. 2004;146(1-2):11-31.
132. Li N, Zhai Y, Zhang Y, Li W, Yang M, Lei J, et al. Structure of the eukaryotic MCM complex at 3.8 Å. *Nature*. 2015;524(7564):186-91.
133. Pierce BG, Wiehe K, Hwang H, Kim BH, Vreven T, Weng Z. ZDOCK server: interactive docking prediction of protein-protein complexes and symmetric multimers. *Bioinformatics*. 2014;30(12):1771-3.
134. Aggarwal M, Sommers JA, Shoemaker RH, Brosh RM, Jr. Inhibition of helicase activity by a small molecule impairs Werner syndrome helicase (WRN) function in the cellular response to DNA damage or replication stress. *Proceedings of the National Academy of Sciences of the United States of America*. 2011;108(4):1525-30.
135. Gupta R, Brosh RM, Jr. Helicases as prospective targets for anti-cancer therapy. *Anti-cancer agents in medicinal chemistry*. 2008;8(4):390-401.
136. Popuri V, Croteau DL, Brosh RM, Jr., Bohr VA. RECQ1 is required for cellular resistance to replication stress and catalyzes strand exchange on stalled replication fork structures. *Cell cycle*. 2012;11(22):4252-65.
137. Suhasini AN, Brosh RM, Jr. Mechanistic and biological aspects of helicase action on damaged DNA. *Cell cycle*. 2010;9(12):2317-29.
138. Koonin EV. A common set of conserved motifs in a vast variety of putative nucleic acid-dependent ATPases including MCM proteins involved in the initiation of eukaryotic DNA replication. *Nucleic acids research*. 1993;21(11):2541-7.
139. Labib K, Tercero JA, Diffley JF. Uninterrupted MCM2-7 function required for DNA replication fork progression. *Science*. 2000;288(5471):1643-7.

140. Aparicio OM, Weinstein DM, Bell SP. Components and dynamics of DNA replication complexes in *S. cerevisiae*: redistribution of MCM proteins and Cdc45p during S phase. *Cell*. 1997;91(1):59-69.
141. Ketchandji M, Kuo YF, Shahinian VB, Goodwin JS. Cause of death in older men after the diagnosis of prostate cancer. *Journal of the American Geriatrics Society*. 2009;57(1):24-30.
142. Brenner JC, Chinnaiyan AM. Disruptive events in the life of prostate cancer. *Cancer cell*. 2011;19(3):301-3.
143. Shembade N, Parvatiyar K, Harhaj NS, Harhaj EW. The ubiquitin-editing enzyme A20 requires RNF11 to downregulate NF-kappaB signalling. *The EMBO journal*. 2009;28(5):513-22.
144. Lee TL, Shyu YC, Hsu TY, Shen CK. Itch regulates p45/NF-E2 in vivo by Lys63-linked ubiquitination. *Biochemical and biophysical research communications*. 2008;375(3):326-30.
145. Farrell J, Kelly C, Rauch J, Kida K, Garcia-Munoz A, Monsefi N, et al. HGF induces epithelial-to-mesenchymal transition by modulating the mammalian hippo/MST2 and ISG15 pathways. *Journal of proteome research*. 2014;13(6):2874-86.
146. Kumar S, Park SH, Cieply B, Schupp J, Killiam E, Zhang F, et al. A pathway for the control of anoikis sensitivity by E-cadherin and epithelial-to-mesenchymal transition. *Molecular and cellular biology*. 2011;31(19):4036-51.
147. Petrova YI, Schecterson L, Gumbiner BM. Roles for E-cadherin cell surface regulation in cancer. *Molecular biology of the cell*. 2016;27(21):3233-44.

148. Garcia-Flores M, Casanova-Salas I, Rubio-Briones J, Calatrava A, Dominguez-Escrig J, Rubio L, et al. Clinico-pathological significance of the molecular alterations of the SPOP gene in prostate cancer. *European journal of cancer*. 2014;50(17):2994-3002.
149. Kuriyan KW. *The Molecules of Life*: Garland Publishing; 2009.
150. Litwin MS, Tan HJ. The Diagnosis and Treatment of Prostate Cancer: A Review. *Jama*. 2017;317(24):2532-42.
151. Raghavan D. First-line use of novel hormonal agents in prostate cancer: a critical appraisal. *Clinical advances in hematology & oncology : H&O*. 2018;16(4):289-95.

APPENDIX A

Approval For Animal Research By Collaborators

西安交通大学动物实验伦理审查批准书 No. XJTULAC2017-781				
Xi'an Jiaotong University Approval for Research Involving Animals				
批准日期 (App. Date): 2017年02月01日 (YY-MM-DD): 2017-02-01				
项目主持人姓名 Name of Principal Investigator	Jinlu Ma	申请人单位 Department	The first affiliated hospital of Xi'an Jiaotong University	
课题名称 Project Title	中央高校基本科研业务费 The Fundamental Research Funds for the Central Universities			
课题来源和批号 (Funding Source & Number)	2013jghz30			
使用动物情况 Animal Requirements	动物来源 Source	Beijing Experimental Animal Center	品种品系 Species or Strains	Athymic nude mice
	数量 Quantity	74只 (♀ 只; ♂74只)		
Animal Requirements	计划开始日期 (Proposed Date of Commencement)	2017-03	计划结束日期 (Proposed Date of Completion)	2017-12
	1. 该项目的实施是否符合 NIH 和学校动管会相关规定。(Are all procedures to be performed in accordance with the 'Principles of Laboratory Animal Care'(NIH) and guidelines of the laboratory animal care committee of Xi'an Jiaotong University.) 2. 所使用的动物品种、等级、规格是否合适, 使用数量的计算依据。(The species, strains, grade, specification and number of the animals to be used should be justified.) 3. 能否通过改良设计方案替代或减少使用所用动物。(Rational for animal use should be justified, including the alternatives to animal use, a refined study design to replace or reduce animal number to be used.) 4. 实验操作中是否善待动物, 包括合理的实验终点、麻醉方案, 不麻醉的理由及减少相应动物痛苦的措施, 实验结束动物的处理, 动物安乐死方案等。(Appropriate animal care and handling throughout the experiment, including a scientific sound endpoint; anesthetics, analgesics, sedatives or tranquilizers that are to be used; explanation for any procedure cause unrelieved pain or distress; disposition of animals at end of study; and euthanasia criteria and method.) 5. 是否使用对人体或环境有害试剂, 有潜在感染性试剂, 放射性物质, 是否使用遗传修饰试剂, 是否进行遗传操作, 相应的防护措施。(Are the materials to be used harmful or toxic? Are there any radioactive agents, infectious agents, genetic modified agents, and the genetic manipulation to be used in the experiment? If yes, the safety measures should be specified.)			
审查项目 Considerations Ethical				
实验动物管理委员会意见 Comments of the laboratory animal care committee				
	代表签名:  Name of Ethics Committee Representative			
	Date: 2017-2-1			

APPENDIX B

Approval For Human Studies By Collaborator

西安交通大学医学院第一附属医院

伦理委员会审查批件

批件号：2010伦理科学第(G-231)号

项目名称	前列腺癌相关基因检测分析				
项目来源	西安交通大学基本科研业务费				
项目负责人	马瑾璐				
审查方式	快速审查 <input type="checkbox"/> 会议审查 <input checked="" type="checkbox"/>				
送审材料	1. 伦理审查申请表 2. 项目申请书 3. 知情同意书				
审查结论	同意	作必要修正后 同意	作必要修正后 重审	不同意	终止或 暂停
	√				
<p>伦理会意见：</p> <p>经过伦理会审查，符合伦理原则，同意在院内开展本研究。</p> <p>主任委员：  时间：2010年6月3日</p>					
注意	<p>1. 对已批准的临床研究方案、知情同意书等材料的任何修改及主要研究者更换等，请及时通知本伦理委员会重新审查，获得批准后执行。</p> <p>2. 本审查结果只涉及对伦理问题的审查结论，如相关研究要求办理相应手续，如到上级部门办理审批/备案手续，或按医院要求需要签署合同书/协议书的，请在项目开展前先行办理上述手续。</p>				